CHEMISTRY
A European Journal

A Journal of
ChemPubSoc Europe

Accepted Article

Title: Magnesium Stung by Non-Classical Scorpionate Ligands: Synthesis and Cone Angle Calculations

Authors: Reiner Anwander, Christoph Stuhl, and Cäcilia Maichle-Mössmer

To be cited as: *Chem. Eur. J.* 10.1002/chem.201803067

Link to VoR: http://dx.doi.org/10.1002/chem.201803067

Supported by
ACES

WILEY-VCH

10.1002/chem.201803067

WILEY-VCH

FULL PAPER

Magnesium Stung by Non-Classical Scorpionate Ligands: Synthesis and Cone Angle Calculations

Christoph Stuhl,[a] Caecilia Maichle-Mössmer,[a] and Reiner Anwander*[a]

Abstract: A series of tris(pyrazolyl)alkane scorpionate ligands of the type $RCTp^{3\text{-}R'}$ (R = Me, *n*Bu, $SiMe_3$; R' = H, Me, Ph, *i*Pr, *t*Bu) was synthesized and their ability to coordinate magnesium methyl moieties was examined. The reaction of $Mg(AlMe_4)_2$ with neutral proligands $HCTp^{3\text{-}Ph}$ or $Me_3SiCTp^{3\text{-}Me}$, containing a non-innocent backbone methine moiety, led to deprotonation/rearrangement and $SiMe_3/AlMe_3$ exchange to afford $[(Me_3AlCTp^{3\text{-}Ph})_2Mg]$ and $[(Me_3AlCTp^{3\text{-}Me})Mg(AlMe_4)]$, respectively, with monoanionic tripodal ligands. Treatment of sterically less demanding $RCTp^{3\text{-}R'}$ with $Mg(AlMe_4)_2$ produced isostructural dicationic "metal-in-a-box" complexes of the type $[(RCTp^{3\text{-}R'})_2Mg][AlMe_4]_2$ (R = Me, *n*Bu; R' = H, Me). Utilization of the superbulky ligands $MeCTp^{3\text{-}Ph}$ and $MeCTp^{3\text{-}t\text{Bu}}$ gave monocationic complexes $[(MeCTp^{3\text{-}Ph})MgMe][AlMe_4]$ and $[(MeCTp^{3\text{-}t\text{Bu}})MgMe][Al_2Me_7]$ as separated ion pairs. The reaction of $Mg(AlMe_4)_2$ with $n\text{BuCTp}^{3\text{-}Ph}$ led to the formation of the dimagnesium complex $[\{(n\text{BuCTp}^{3\text{-}Ph})Mg(AlMe_4)\}_2(\mu\text{-}CH_3)]$, featuring a bridging methyl moiety and terminal η^1-coordinated tetramethylaluminato ligands. Isopropyl-substituted ligand $MeCTp^{3\text{-}i\text{Pr}}$ emerged from further fine-tuning of the steric and electronic parameters and when reacted with $Mg(AlMe_4)_2$ gave $(MeCTp^{3\text{-}i\text{Pr}})Mg(AlMe_4)_2$, representing the first example of a magnesium bis(alkyl) complex with an intact $RCTp^{3\text{-}R'}$ ligand. The exact ligand cone angles of all magnesium complexes were determined according to the mathematical analysis developed by Allen et al.

Introduction

Organomagnesium compounds, and in particular Grignard reagents [RMgX] (R = alkyl, X = halogenido), belong to the most popular and most studied organometallic reagents.[1] Ongoing immense interest is emphasized by a rapidly growing library of magnesium alkyl complexes bearing multidentate N- and O-chelating ligands, which routinely displace the halogenido ligand X.[2] Several types of scorpionate ligands have been employed in an effort to stabilize monomeric complexes[3] and to counteract the Schlenk equilibrium.[4] The classical Trofimenko ligand[5] and polypyrazolyls with different main group elements in the bridging position (Al,[6] Ga,[7] C[8], Si[9] or P[10]), as well as tridentate ligands with different heterocycles[11] or hybrid scorpionates[12] can efficiently encapsulate the magnesium center and protect from agglomeration.[8,9b,10,13] According to the concepts of modern coordination chemistry such scorpionates display highly versatile ligand scaffolds the steric and electronic properties of which can be efficiently fine-tuned by varying the substituents of the pyrazole and the central boron or carbon atom linking the heterocycles.[14]

[a] Institut für Anorganische Chemie, Eberhard Karls Universität Tübingen, Auf der Morgenstelle 18, 72076 Tübingen, Germany
E-Mail: reiner.anwander@uni-tuebingen.de
http://uni-tuebingen.de/syncat-anwander

Supporting information for this article is given via a link at the end of the document.

Overall, the synthesis approaches to magnesium tris(pyrazolyl)methane or -methanide complexes seem limited to (1) protonolysis of Grignard reagents or reactive organomagnesium complexes by the methine C−H moiety affording mono- or bis-methanide complexes **I** and **II** (Chart1), (2) reprotonation of the methanide moiety by a Brønsted acid generating **III** or **IV**, respectively, and (3) Lewis acid−base reactions of methanide sandwich complexes with organoaluminum reagents giving trimetallic $MgAl_2$ complexes **V**. Furthermore, alkaline-earth metal methanide complexes can degrade via C−N bond cleavage to form pyrazolate complexes.[15] Breher and Mountford have comprehensively examined reactions of alkaline-earth metal complexes with tris(pyrazolyl)methanes,[14b,14c] while the proneness of the methine moiety for C–H bond activation in the presence of a strong base was particularly emphasized.[14b] Tris(pyrazolyl)methane (HCTp) was initially synthesized by Hückel in 1937, by treating chloroform with potassium pyrazolate (Kpz).[16] Later on, Elguero applied a phase transfer catalysis to access the desired tris(3-R-pyrazolyl)methane derivatives $HCTp^{3\text{-}R}$ (R = H, Me, Ph, *i*Pr, *t*Bu), but had to deal with mixtures of four structural isomers.[17]

We have recently embarked on the feasibility of well-defined magnesium alkyl species.[18] For example, the reaction of hydrotris(pyrazolyl)borate $KTp^{Me,Me}$ with dimethylmagnesium or $Mg(AlMe_4)_2$, initially described by Ziegler in 1957,[19] afforded the terminal hydrocarbyls $[(Tp^{Me,Me})MgMe]$ and $[(Tp^{Me,Me})Mg(AlMe_4)]$.[4] Interestingly, polymeric $[MgMe_2]_n$ and bimetallic $Mg(AlMe_4)_2$ can be mutually interconverted by either

addition of organoaluminum reagent or diethyl ether, clearly being reminiscent of the donor-induced tetraalkylaluminate cleavage of $Ln(AlMe_4)_3$ into $[LnMe_3]_n$ (Ln= Y, Ho, Lu).[20] Moreover, the tris(pyrazolyl)borato ligand can stabilize reactive rare-earth metal hydride, alkyl, imide or methylidene complexes.[21] Spurred by these findings we set out to elaborate the chemistry of neutral tris(pyrazolyl)alkane ligands RCTp with organomagnesium compounds. It was evident from the previous studies that the feasibility of discrete magnesium alkyl complexes will require more resilient backbone C–R functional groups. Herein, we systematically extend the limited library of neutral symmetrical tris(pyrazolyl) scorpionates of the general type $RCTp^{3\text{-}R'}$ and assess the reactivity toward highly reactive magnesium methyl complexes.

For a comprehensive understanding of the structural diversity in magnesium tris(pyrazolyl)alkane and -methanide complexes the Tolman cone angles were calculated by adopting the mathematical model, which was extensively studied for phosphine ligands coordinating to nickel.[22] Trofimenko applied this concept to tris(pyrazolyl)borato ligands, but at that time several restraints have been introduced such as fixed metal ligand atom distances or by selecting distinct ligand atoms for the calculations which resulted in significant deviations from the mathematically exact ligand cone angle.[23] Allen and his group developed a mathematical analysis in order to determine the right cone axis from the experimental crystal data with major implications for structure-reactivity correlations, e.g., in kinetic studies and catalysis.[24] The present cone angle calculation is therefore performed according to Allen et al.[24]

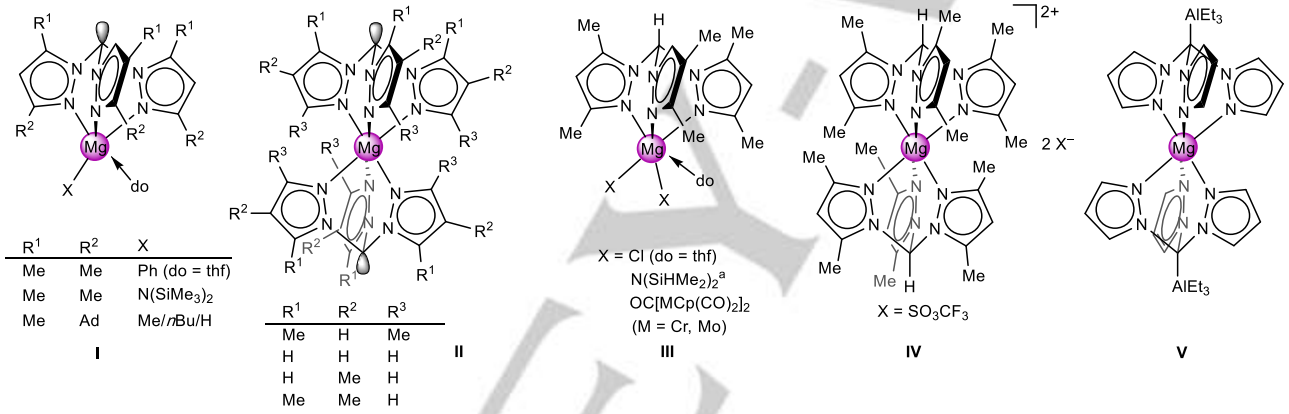

Chart1. Structurally characterized tris(pyrazolyl)methane and -methanide magnesium complexes (a κ^2(N,N') mode)

Results and discussion

Tris-3-alkylpyrazolylalkane $RCTp^{3\text{-}R'}$ Ligand Synthesis and Library. Crucial criteria for the ligand selection were enhanced solubility/cone angle variation and ligand backbone modification. The former two are routinely achieved via derivatization of the pyrazolyl rings with alkyl and aryl groups. Functionalization of the apical methine carbon atom provides protection against nucleophilic attack. Substitution of the pyrazolyl rings in 3-position is efficient for such tripodal ligands with respect to fine-tuning of the ligand cone angle. Routinely, the $RCTp^{3\text{-}R'}$ ligands coordinate to metal centers in a κ^3(N,N',N'') fashion, through three nitrogen atoms, but other coordination modes such as the κ^2(N,N') mode with either an intermolecular bridging pyrazolyl ring or one non-coordinating/dangling pyrazolyl moiety have been reported as well.[25] Figure 1 shows the selection of tris(3-alkylpyrazolyl)alkane ligands used in this study. The tris(3-alkylpyrazolyl)methane precursors $HCTp^{3\text{-}R'}$(**2**) were synthesized from the parent pyrazoles (**1**)[23,26] by applying Elguero's phase transfer catalysis protocol, which generates a mixture of complex isomers.[17] The ratios of the isomeric mixture can be optimized by refluxing in toluene and via addition of catalytic amounts of *p*TsOH, promoting the formation of the symmetric species **2** (see Scheme 1). As the C–H methine backbone requires substitution with a more resilient group, the reaction mixture is lithiated with *n*BuLi or $Li[N(SiMe_3)_2]$, respectively, generating $LiCTp^{3\text{-}R'}$. Subsequent *in situ* addition of alkyl halides R-X affords the neutral $RCTp^{3\text{-}R'}$ (**3**) via nucleophilic substitution.[27] Compounds **3** were purified by recrystallization, if not otherwise stated, and **3d**-**3k** have been characterized by single-crystal X-ray diffraction analyses (see Supporting Information). The synthesis route is efficient for the preparation of a variety of functionalized ligands $RCTp^{3\text{-}R'}$ (R = Me, *n*Bu, Me_3Si, Bn; R' = H, Me, Ph, *i*Pr, *t*Bu). In this study we were able to add five new ligands to the library of neutral pyrazolyl alkane ligands,[28] *n*BuCTp (**3b**), nBuCTp$^{3\text{-Me}}$ (**3e**), $Me_3SiCTp^{3\text{-Me}}$ (**3f**), nBuCTp$^{3\text{-Ph}}$ (**3h**) and $MeCTp^{3\text{-}i\text{Pr}}$ (**3j**) (Figure 1).

10.1002/chem.201803067

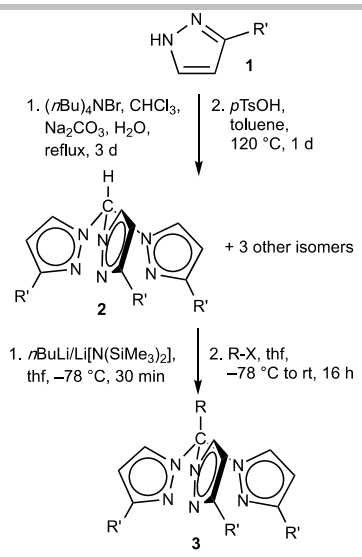

Scheme 1. Synthesis of RCTp$^{3\text{-}R'}$ Ligands **3** via Phase Transfer Catalysis of 3-Substitued Pyrazoles and Electrophilic Backbone Substitution**.**

Choice of Magnesium Methyl Precursor. Pre-screening Studies. Since non-coordinating aliphatic or aromatic solvents were envisioned as the most appropriate for the synthesis of the targeted discrete organomagnesium tris(pyrazolyl)alkane complexes of the type [RCTp$^{3\text{-}R'}$]MgR$_2$, bis(tetramethyl)aluminate complex Mg(AlMe$_4$)$_2$ was selected as a well-defined, highly soluble metal precursor.[19,29] A pre-screening study with [MgMe$_2$]$_n$ revealed that not only the methine moiety of tris(pyrazolyl)methane **2** gets readily deprotonated by this strong base, which is in agreement with previously reported respective reactivity of Mg*n*Bu$_2$ or MeMgX,[14b,14c] but also the functionalized alkane ligands RCTp$^{3\text{-}R'}$ (**3**) suffer from degradation. Monitoring reaction mixtures of sterically less demanding ligands **3** with [MgMe$_2$]$_n$ (**4**) in equimolar ratios by ^{1}H NMR spectroscopy in [D$_6$]benzene or [D$_8$]thf, indicated decomposition of the RCTp ligands within minutes (**3a**-**c**) up to several weeks (**3d**-**f**). This degradation process appeared interesting since it might indeed hint to transient species "(RCTp)MgMe$_2$", which would then undergo decomposition. To gain further insight into the decomposition process of putative (RCTp)MgMe$_2$ a series of experiments was performed. On one occasion, by reacting **4** with **3c** in a dme/thf mixture at −40 °C, colorless cuboid crystals of [(dme)(thf)Mg(pz)$_3$MgMe] (**5**) formed, suitable for analysis by X-ray diffraction (Figure 2, monoclinic, *P*2$_1$/*n*).

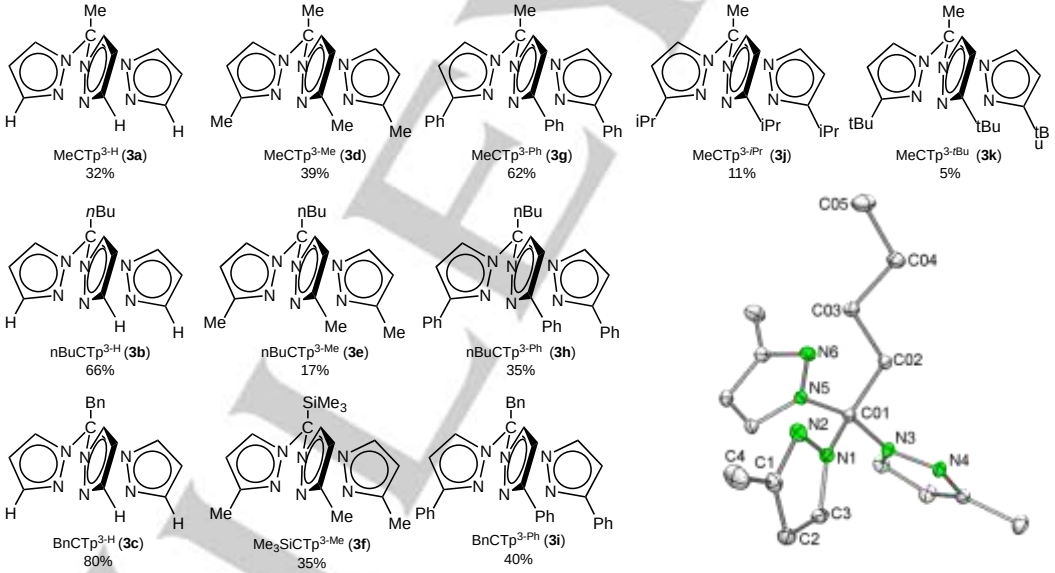

Figure 1. Overview of RCTp ligands with overall yields, starting from 1-*H*-pyrazole (**3a-c**), 3-Me-pyrazole (**3d-f**), acetophenone (**3g-i**)[26b], 3-methylbutan-2-one (**3j**)[23], pinacolone (**3k**)[26a]. Representative solid-state structure of **3e**. X-ray structure analyses were performed on tris(pyrazolyl)alkane ligands **3d-3k** (see Supporting Information).

The metal centers in dimagnesium complex **5** are bridged by three pyrazolyl ligands in μ_2-η^1:η^1 fashion. Mg2 adopts an octahedral geometry by accommodating additionally one thf and one dme molecule, with the [Mg(thf)(dme)] moiety replacing the former CBn backbone moiety. Atom Mg1 features one terminal methyl group, suggesting the initial coordination of the intact ligand to dimethylmagnesium. The Mg–C bond length of 2.131(2) Å is similar to four-coordinate **4a** (vide infra) and is

10.1002/chem.201803067

significantly shorter in comparison to the metrical parameter in **4b** (CN 5, vide infra). Moreover, complex **5** shows distinctly different Mg–N bond distances of av. 2.087 Å (Mg1–N = 2.076(2)-2.106(2) Å) and 2.153 Å (Mg2–N = 2.137(2)-2.175(2) Å). For comparison, the Mg–N(μ_2-pz) bond lengths of av. 2.024 Å in four-coordinate Mg_2(pz-*t*Bu_2-3,5)$_4$ are slightly shorter.[30] The isolation of **5** indicates that the C–N bonds of the tris(pyrazolyl)methane ligands are still susceptible to attack by strong nucleophiles (Scheme 2, transition state): The feasibility of a reaction intermediate as shown in Scheme 2 is further corroborated by the existence of magnesates, such as $[Mg_2Me_5]^-$ or $[Mg_3Me_8]^{2-}$.[31]

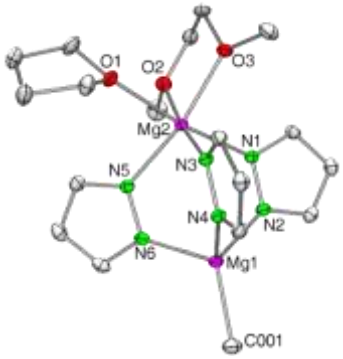

Figure 2. Solid-state structure of complex [(dme)(thf)Mg(pz)$_3$MgMe] (**5**). Hydrogen atoms have been omitted for clarity. Atomic displacement ellipsoids are set at the 50% probability level.

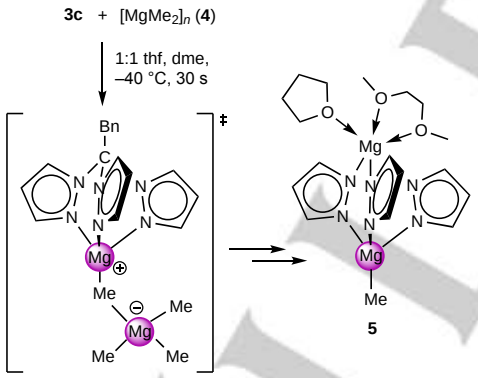

Scheme 2. Proposed Scenario for the Formation of [(dme)(thf)Mg(pz)$_3$MgMe] (**5**).

For the synthesis of $Mg(AlMe_4)_2$,[19] we attempted to optimize the reaction conditions starting from two different Grignard reagents, namely [MeMgBr] and [MeMgCl] (Scheme 3). Shifting the [MeMgBr]-Schlenk equilibrium by the addition of 1,4-dioxane, polymeric [$MgMe_2$(dioxane)]$_n$ (**4a**) was isolated upon separation of solid [$MgBr_2$(dioxane)].[32] Single crystals of **4a** suitable for diffraction analysis were grown from saturated solutions of [$MgMe_2$]$_n$ (**4**) in 1,4-dioxane. The perspective view of complex **1a** (orthorhombic, *Cmcm*) is depicted in Figure 3. For comparison, the Mg–C bond length of 2.135(1) Å is similar to the metrical parameters in isostructural dialkylmagnesium 1,4-dioxane polymers of the general type [MgR_2(dioxane)]$_n$ (Mg–C [Å]: R = Et, 2.142(2); R = *i*Pr, 2.157(2); R = Np, 2.133(2); R = Ph, 2.135(2); R = Bn, 2.156(2) / 2.155(2))[33].

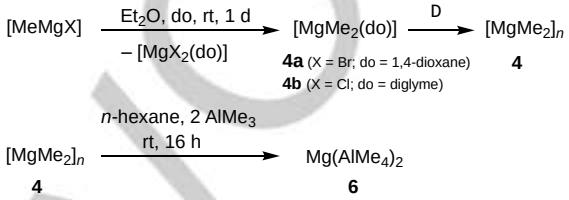

Scheme 3. Synthesis of $Mg(AlMe_4)_2$ (6) from Grignard Reagents.

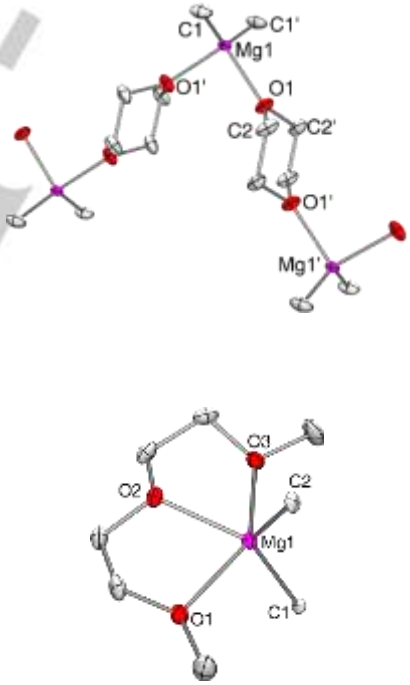

Figure 3. Solid-state structure of polymeric **4a** (top) and monomeric **4b** (bottom). Hydrogen atoms have been omitted for clarity. Atomic displacement ellipsoids are set at the 50% probability level.

The reaction of [$MeMgCl(thf)_2$] with tridentate donor ligand bis(2-methoxyethyl)ether (diglyme) afforded magnesium complex [$MgMe_2$(diglyme)] (**4b**). Its solid-state structure revealed a 5-coordinate magnesium center surrounded by three diglyme oxygen atoms und two methyl carbon atoms. As expected, the Mg–C(CH_3) bond lengths of 2.193(2) and 2.197(2) Å are slightly elongated in comparison to the ones found in polymeric

10.1002/chem.201803067

$[MgMe_2(1,4\text{-dioxane})]_n$ with 4-coordinate magnesium (vide supra). The isolation and purification of **4** via thermal treatment of **4b** in vacuum is hampered by the high boiling point of diglyme (186 °C). Decomposition of **4b** started at temperatures >100 °C and despite several drying cycles, remaining diglyme was indicated by ^{1}H NMR spectroscopy. The absence of diglyme in **4** is a crucial factor for synthesizing $Mg(AlMe_4)_2$ (**6**) as for comparison undesired separated ion pair $[Mg(thf)_6][AlMe_4]_2$ was shown to form by treating **6** with thf.[18a] Finally, the purest samples of donor-free $[MgMe_2]_n$ (**4**) were obtained by de-solvating 1,4-dioxane adduct **4a** under high vacuum (10^{-4} mbar) at 130 °C,[34] and used for the synthesis of $Mg(AlMe_4)_2$ (**6**) by standard procedures (Scheme 3).[35]

Reactivity of $Mg(AlMe_4)_2$ towards $RCTp^{3\text{-}R'}$ (Scheme 4). The main emphasis of this study was to examine the steric and electronic implications of the tris(pyrazolyl)alkanes for the coordination to magnesium and the stabilization of reactive alkyl magnesium complexes by steric protection. In order to avoid extensive backbone functionalization and nucleation to highly aggregated Mg/Al complexes it is essential that the RCTp ligand stays neutral. As expected, only RCTp ligands with a resilient C–R backbone are suitable for accommodating **6**. For example, the reaction of methylaluminate **6** with $HCTp^{3\text{-}Ph}$ (**2-Ph**) led to the isolation of magnesium bis(methanide) complex **7** via displacement of the methine hydrogen by $AlMe_3$ under elimination of methane. In **7**, the magnesium metal center is encapsulated by two anionic $Me_3AlCTp^{3\text{-}Ph}$ scaffolds to yield $(Me_3AlCTp^{3\text{-}Ph})_2Mg$ as a neutral "metal-in-a-box" complex (Figure 4, tetragonal, $P4_2/n$). The same structural motif was previously observed for $(Et_3AlCTp^{3\text{-}H})_2Mg$ (**V**, Chart 1). The ^{1}H NMR spectrum of **7** shows two doublets at 8.90 and 5.86 ppm for the 4- and 5-pyrazolic protons and one singlet at 0.26 ppm for the $AlMe_3$ groups.

A similar product was isolated from the equimolar reaction of **3** with $Me_3SiCTp^{3\text{-}Me}$ (**3f**) under elimination of $SiMe_4$. The initial suspension cleared up and afforded neutral complex $(Me_3AlCTp^{3\text{-}Me})Mg(AlMe_4)$ (**8**, Figure 5, monoclinic, $P2_1/c$). In accordance with **7** the ^{1}H NMR spectrum of **8** in [D$_6$]benzene revealed two doublets for the pyrazolic protons at 8.49 and 5.31 ppm, indicating equivalent pyrazolyl anchors. One sharp singlet at 0.02 ppm for $AlMe_3$, κ^1-coordinated by the methanide carbon, and one singlet at –0.19 ppm for the $[AlMe_4]$ moiety was observed. In the solid state, the magnesium center adopts a distorted octahedral geometry, with the anionic methanide ligand coordinating in a tripodal κ^3(N,N',N'') fashion (av. Mg−N, 2.125 Å). The Mg···Al distance of 2.595(1) Å and Mg–C bond lengths (2.501(2)-2.680(2) Å) of the η^3-coordinated $[AlMe_4]$ unit are in average shorter than the metrical parameters in $(Tp^{Me,Me})Mg(AlMe_4)$ (Mg–C, 2.434(2)-2.853(2) Å, Mg···Al, 2.676(1) Å, Mg–N, 2.079(2)-2.115(2) Å).[4] The Al2–C01 bond lengths are 2.203(1) Å for **7** and 2.189(1) Å for **8**, comparable to the Al–C bond distance of 2.178(2) Å in $(Et_3AlCTp^{3\text{-}H})_2Mg$.[14c]

The reactions of **6** with benzyl-substituted tris(pyrazolyl) methane ligands **3c** and **3i**, prone to backbone cleavage, led to multiple decomposition products.

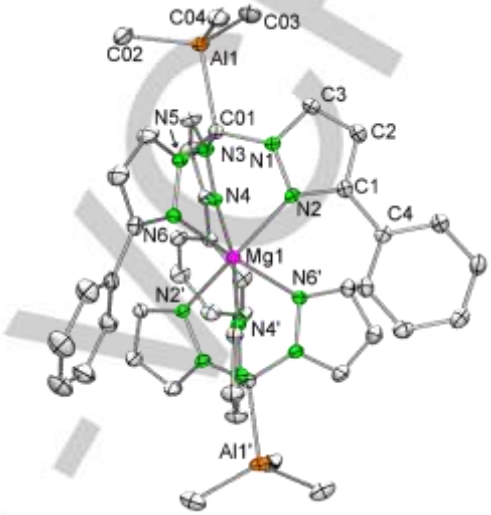

Figure 4. Solid-state structure of **7**. Hydrogen atoms and the phenyl groups of the second lower $Me_3AlCTp^{3\text{-}Ph}$ ligand are omitted for clarity. Atomic displacement ellipsoids are set at the 50% probability level.

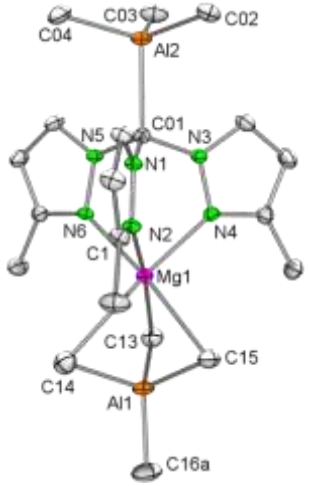

Figure 5. Solid-state structure of **8**. Hydrogen atoms are omitted for clarity. Atomic displacement ellipsoids are set at the 50% probability level.

10.1002/chem.201803067

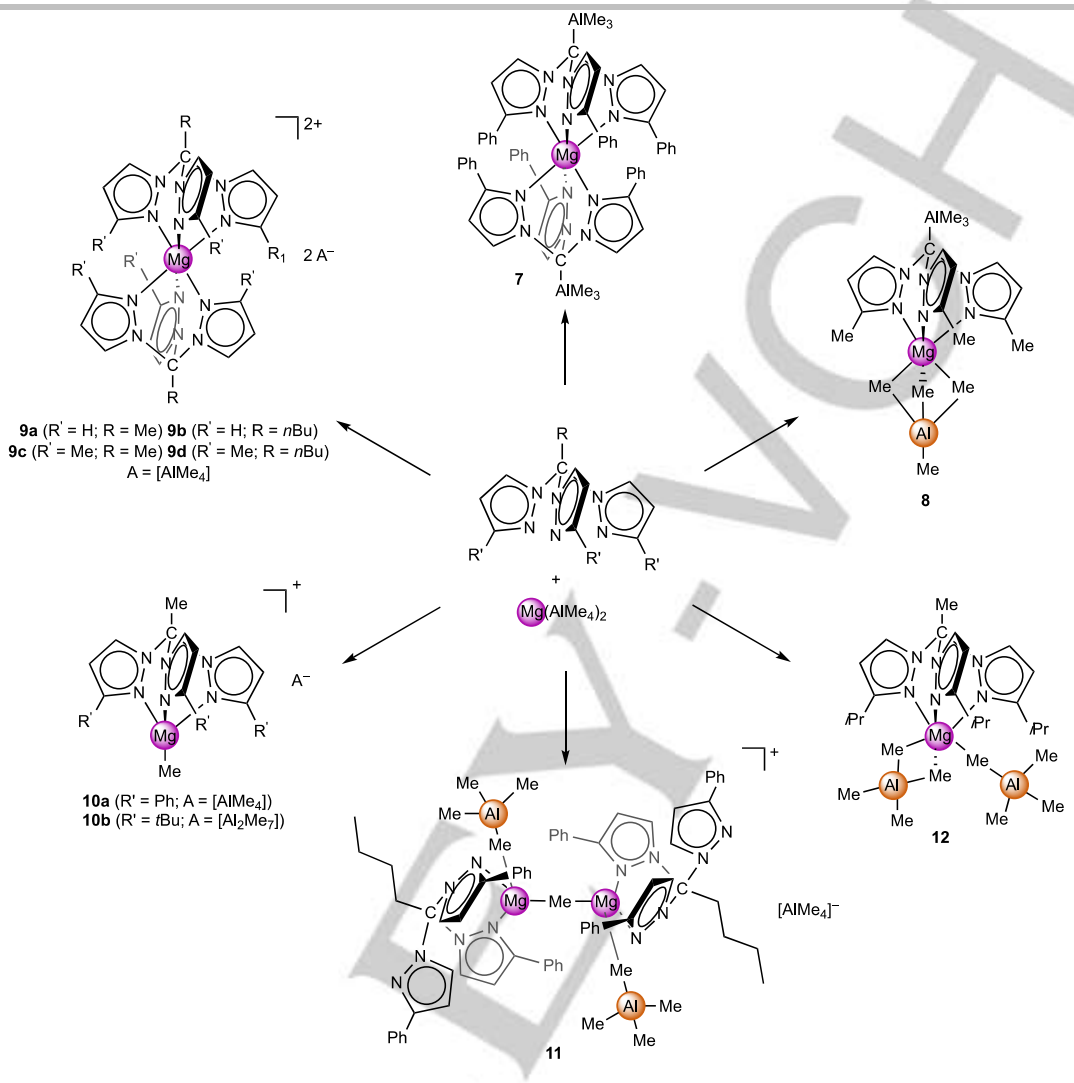

Scheme 4. Synthesis of Tris(pyrazolyl)alkane and -Methanide Complexes **7**-**12**.

Toluene/*n*-hexane solutions of ligands **3** (**3a**-**b**, **3d**-**e**) and **6** in 2:1 ratios caused instant precipitation of white powders in quantitative yields. When the powders were dissolved in thf fast decomposition was observed. However, rapid handling and immediate removal of thf by evaporation gave clear colorless single crystals. X-Ray crystallographic analyses indicated the formation of separated ion pairs $[(RCTp)_2Mg][AlMe_4]_2$ (**9a**-**d**, Figure 6). The molecular structures of **9a**-**d** revealed six-coordinate magnesium centers with two tris(pyrazolyl)alkane ligands in κ^3(N,N',N'') modus, adopting a distorted octahedral geometry. The Mg–N bond lengths lie in the expected range of similar magnesium tris(pyrazolyl)alkane compounds (Table 1).[3b,10,14b,14c,15,36]

Complexes **9** are insoluble in non-coordinating solvents, but dissolve readily in thf. The κ^3(N,N',N'') coordination of the ligands observed in the solid-state of the separated ion pairs **9** is labile since two or three sets of signals for backbone and pyrazolyl moieties are indicated by ^{1}H and ^{13}C{^{1}H} NMR spectroscopy in thf-d_8. The resonances can be assigned to ion pairs **9**, free ligand and mono tris(pyrazolyl)alkane complex $[(RCTp)MgMe(thf)_2][AlMe_4]$ (cf., supporting information). A coupling constant of $^1J_{Al-C}$ = 70.2 Hz was observed in the ^{13}C{^{1}H} NMR spectrum of **9b** (**9d**, 72.5 Hz), which is attributed to the anionic $[AlMe_4]^-$ fragment, in accord with the spectroscopic data of similar complexes.[37]

10.1002/chem.201803067

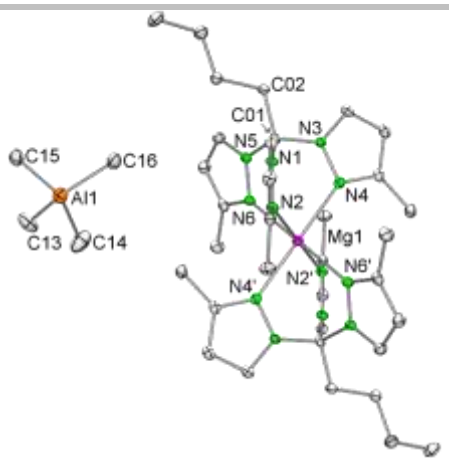

Figure 6. Solid-state structure of separated ion pair [(*n*BuCTp$^{3\text{-Me}}$)$_2$Mg][AlMe$_4$]$_2$ (**9d**). Complexes **9a**, **9b**, and **9c** are isostructural and shown in the Supporting Information. One [AlMe$_4$]$^-$ anion and hydrogen atoms are omitted for clarity. Atomic displacement ellipsoids are set at the 50% probability level.

Treatment of **6** with superbulky MeCTp$^{3\text{-Ph}}$ (**3g**) or MeCTp$^{3\text{-}t\text{Bu}}$ (**3k**, "*tetrahedral enforcer*"), gave separated ion pairs [(MeCTp$^{3\text{-Ph}}$)MgMe][AlMe$_4$] (**10a**, 64%, Θ° = 283), and [(MeCTp$^{3\text{-}t\text{Bu}}$)MgMe][Al$_2$Me$_7$] (**10b**, 91%, Θ° = 275) with one ligand coordinating to the [MgMe]$^+$ cation. By providing the substituents in the 3-position of the pyrazoles with aryl and alkyl groups the solubility was significantly enhanced. Single crystals of **10** were grown from either hot toluene solutions by slow cooling to ambient temperature or toluene/1,2-difluorobenzene mixtures. X-ray diffraction studies confirmed the cationization of isostructural complexes **10a** (Figure 7, top) and **10b** (Figure 7, bottom), while the anionic units are serendipitously [AlMe$_4$] or [Al$_2$Me$_7$]. The Mg–C(methyl) bond lengths of 2.091(2) Å (**10a**) and 2.115(2) Å (**10b**) are relatively short and similar to those in [(Tp$^{\text{Me,Me}}$)MgMe] (2.097(4) Å) or [(Tp$^{t\text{Bu,Me}}$)MgMe] (2.119(3) Å).[36d] For further comparison, the Mg–C(CH$_3$) bond distances in four-coordinate magnesium complexes [(SiMe$_3$ArN)MgMe(thf)$_2$][38] are in the range of 2.129(4) to 2.173(4) Å.

The ^{1}H NMR spectrum of **10a** in [D$_6$]benzene/1,2-difluorobenzene (1,2-DFB) displays doublets at 7.94 and 6.12 ppm for the 4- and 5-pyrazolic protons indicating free rotation of the phenyl substituents in solution. However, the broad resonances of the metal-bonded methyl groups at –0.03 ppm (Al–CH$_3$, 12H) and –1.16 ppm (Mg−CH$_3$, 3H) give evidence for strong interactions and redistributions in solution (Figure S28). The ^{1}H NMR spectrum of the *tert*-butyl derivative **10b** in [D$_6$]benzene-*d*$_6$/1,2-difluorobenzene at ambient temperature revealed only one set of signals for the tris(pyrazolyl)methane ligand, indicating the absence of a rotational barrier in solution, and sharp singlets for the Mg−CH$_3$ and [Al$_2$Me$_7$] moieties at −0.35 and −0.22 ppm (Figure S30).

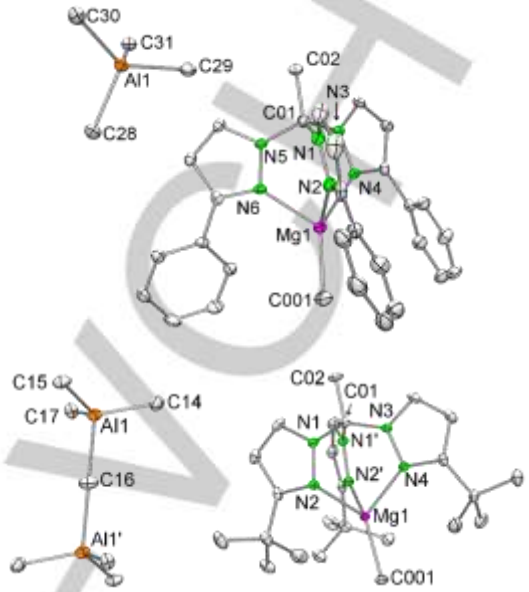

Figure 7. Solid-state structures of separated ion pairs [(MeCTp$^{3\text{-Ph}}$)MgMe][AlMe$_4$] (**10a**, top) and [(MeCTp$^{3\text{-}t\text{Bu}}$)$_2$Mg][Al$_2$Me$_7$] (**10b**, bottom). Hydrogen atoms are omitted for clarity. Atomic displacement ellipsoids are set at the 50% probability level.

Notably, the reaction of **6** with *n*BuCTp$^{3\text{-Ph}}$ (**3h**) led to a very rare κ^2(N',N'') coordination of the ligand. Complex **11** was obtained as colorless crystals from saturated toluene or benzene solutions at ambient temperature. The structural elucidation by X-ray diffraction studies revealed the formation of a monocationic dimagnesium species [{(*n*BuCTp$^{3\text{-Ph}}$)Mg(AlMe$_4$)}$_2$(μ-CH$_3$)] with magnesium centers bridged by one methyl group and [AlMe$_4$] as a counteranion (triclinic $P\bar{1}$). Obviously, the substituent (*n*Bu versus Me) in the backbone carbon has a major impact on the structure in the solid state (monomer **10a** versus dimagnesium species **11**). Each magnesium center in **11** is 4-coordinate by two pyrazolyl nitrogen atoms, a η^1-coordinated [(μ-CH$_3$)Al(CH$_3$)$_4$] fragment and the bridging methyl group. The Mg–C bond lengths of 2.250(2) and 2.209(2) Å in dimagnesium moiety Mg(μ-CH$_3$)Mg are considerably shorter compared to the bridging methyl groups of the η^1-coordinated unit in neutral Mg(μ-CH$_3$)Al(CH$_3$)$_3$ (Mg–C, 2.322(2), 2.337(2) Å). For further comparison, the Mg–C bond lengths of the cationic unit Mg(μ-CH$_3$)Mg in **11** are considerably shorter than in cationic [Mg$_2$(μ-CH$_3$)$_3$(tacn)$_2$]$^+$ (av. Mg–C, 2.355 Å, tacn = N,N',N''-trimethyl-1,4,7-triazacyclononane) or magnesate [Mg$_3$(μ-CH$_3$)$_4$(CH$_3$)$_4$]$^{2-}$ (av. Mg–C, 2.295 Å)[31b], but compare well to neutral [Mg(μ-CH$_3$)(CH$_3$)(thf)]$_2$ (av. Mg–C, 2.263 Å).[18a]

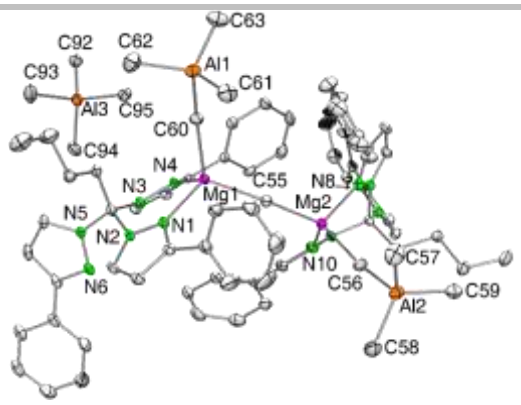

Figure 8. Solid-state structure of dimagnesium species **11**. Lattice solvent and hydrogen atoms are omitted for clarity. Atomic displacement ellipsoids are set at the 50% probability level.

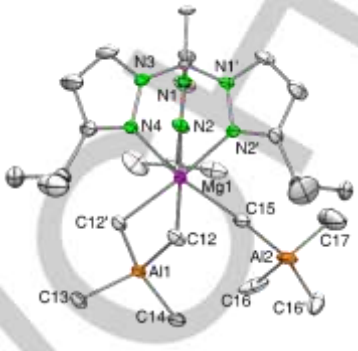

Figure 9. Solid-state structure of compound [(MeCTp$^{3\text{-}iPr}$)Mg(AlMe$_4$)$_2$] (**12**). Hydrogen atoms are omitted for clarity. Atomic displacement ellipsoids are set at the 50% probability level.

The ^{1}H NMR spectrum of **11** in [D$_6$]benzene/1,2-DFB at ambient temperature shows a broad singlet at −0.57 ppm for the methyl groups and one set of broad signals for the tris(pyrazpolyl)pentane ligand, indicating highly fluxional processes in solution. This originates from rapid methyl group exchange and a $\kappa^2 \rightarrow \kappa^3$ coordination shift of *n*BuCTp$^{3\text{-Ph}}$ (**3h**). Further investigations by VT NMR spectroscopy were hampered by the limited solubility of **11** at lower temperatures. Compound **11** is stable against thermal treatment at 80 °C under inert atmospheres. Upon heating to 100 °C resulted generally in the decomposition of the tris(pyrazolyl)alkane ligands **3**.

Finally, the tris(pyrazolyl)ethane ligand MeCTp$^{3\text{-}iPr}$ (**3j**) seems to provide an ideal cone angle (Θ° = 248.76) for Mg(AlMe$_4$)$_2$. The envisaged reaction of **3j** and **6** in *n*-hexane/toluene (1:1) afforded complex [MeCTp$^{3\text{-}iPr}$Mg{(μ_2-Me)AlMe$_3$}{(μ_2-Me)$_2$AlMe$_2$}] (**12**). Single crystals were grown from 1,2-difluorobenzene and X-ray crystallographic studies revealed the formation of the sought-after neutral "(RCTp$^{3\text{-}R'}$)MgR$_2$" motif. The six-coordinate magnesium center in **12** adopts an octahedral geometry with two methyl carbon atoms and two pyrazolyl nitrogen atoms of the κ^3(N,N',N'') coordinated CTp ligand in the equatorial plane and each one nitrogen and carbon atom in the axial positions. As expected, the Mg–C(μ_2-CH$_3$) bond lengths of 2.493(3) and 2.520(5) Å are markedly elongated compared to the Mg–C bond lengths determined by Stucky and coworkers in the donor ligand-free Mg(AlMe$_4$)$_2$ (2.194(9)-2.222(9) Å).[29] The Mg–C15–Al2 bond angle of 175.6(2)° probably indicates the pending formation of a separated ion pair with [AlMe$_4$] as the anionic fragment. Intriguingly, subtle changes of the steric bulk in tripodal tris(pyrazolyl)ethane ligands **3j** and **3k** (*i*Pr versus *t*Bu) entail the formation of ion pair [(MeCTp$^{3\text{-}tBu}$)MgMe][Al$_2$Me$_7$] (**10b**) or neutral [(MeCTp$^{3\text{-}iPr}$)Mg{(μ_2-Me)AlMe$_3$}{(μ_2-Me)$_2$AlMe$_2$}] (**12**), respectively (see Table 1). The tris(pyrazolyl)ethane ligand MeCTp$^{3\text{-}iPr}$ (**3j**) is less encapsulating, but repulsive interactions between the *i*Pr group counteract the formation of a "metal-in-a-box" complex.

The ambient-temperature ^{1}H NMR spectrum of **12** shows two doublets in the aromatic region for the pyrazolyl hydrogen atoms at 7.77 and 5.78 ppm. A very sharp singlet appeared at –0.14 ppm with an integral ratio matching eight methyl groups, indicating rapid exchange of bridging and terminal methyl groups. VT ^{1}H NMR spectroscopic studies of **12** in [D$_8$]toluene revealed that the singlet at –0.14 ppm splits into two dominant and four low-intensity signals at –50 °C (Figures S36 and S37). Moreover, the backbone methyl group appeared as two signals at –40 °C (2:1 ratio). This manifests a very complicated fluxional behavior in solution which might involve species similar to dimagnesium complex **11** and dissociated AlMe$_3$. However, at elevated temperature only one sharp singlet –0.39 ppm could be observed for all methyl ligands, with the dynamic behavior of **12** being fully reversible.

Cone Angle Calculation and Examination. Spurred by the distinct coordination behavior of the tris(pyrazolyl)alkane ligands RCTp$^{3\text{-}R'}$ and the diverse reactivity patterns with Mg(AlMe$_4$)$_2$ we became interested in evaluating the steric effect of the ligands in more detail (Table 1). Although predominantly developed for tertiary phosphines the steric effect of any multipodal ligand can be mathematically described.[24] In previous work, the cone angles were determined, inter alia, by the ligand hydrogen atoms, which are closest to the metal center.[26a,39] In this work, we calculated the cone angles with respect to the shortest magnesium ligand side arm hydrogen distances (Θ), taking into account the van der Waals radii (Θ_{vdw}) or the maximum and "exact" cone angle determined by the Mathematica package (Θ°).[40] The exact procedure is given in the supporting information.[24] Strictly speaking, comparison among the ligands is only feasible, if (a) the metal centers have the same coordination number (CN) and (b) in case of the same overall metal-ligand charge (meaning either dicationic, monocationic or neutral complexes).

Table 1. Overview of Selected Bond Lengths and Cone Angles Θ, Θ_{vdw} and Θ° of Magnesium Tris(pyrazolyl)alkane and -Methanide Complexes as well as Hydrotris(pyrazoyl)borate Derivatives (see Supporting Information for calculations).[a]

	CN	Mg–N2	Mg–N4	Mg–N6	avg. Mg–N	Mg–C01 / Mg–B1	Θ	Θ_{vdw}	Θ°	ref.
$[(Me_3AlCTp^{3\text{-}Ph})_2Mg]$ (**7**)	6	2.256(1)	2.190(1)	2.188(1)	2.211	3.188(1)	218.04	263.06	272.87	b
$[(Me_3AlCTp^{3\text{-}Me})Mg(AlMe_4)]$ (**8**)	5	2.116(1)	2.123(1)	2.138(2)	2.126	3.180(1)	208.41	252.50	252.46	b
$[(MeCTp^{3\text{-}H})_2Mg][AlMe_4]_2$ (**9a**)	6	2.113(1)	2.141(1)	2.138(1)	2.131	3.222(1)	165.42	206.20	206.22	b
$[(n\text{BuCTp}^{3\text{-}H})_2Mg][AlMe_4]_2$ (**9b**)	6	2.127(1)	2.151(1)	2.131(1)	2.136	3.231(2)	165.73	206.66	206.70	b
$[(MeCTp^{3\text{-}Me})_2Mg][AlMe_4]_2$ (**9c**)	6	2.164(1)	2.141(1)	2.164(1)	2.156	3.216(1)	207.58	252.40	252.42	b
$[(n\text{BuCTp}^{3\text{-}Me})_2Mg][AlMe_4]_2$ (**9d**)	6	2.150(1)	2.196(1)	2.160(1)	2.169	3.230(2)	207.45	252.00	252.01	b
$[(MeCTp^{3\text{-}Ph})MgMe][AlMe_4]$ (**10a**)	4	2.138(2)	2.142(2)	2.128(2)	2.136	3.167(3)	217.17	265.78	282.84	b
$[(MeCTp^{3\text{-}t\text{Bu}})MgMe][Al_2Me_7]$ (**10b**)	4	2.125(1)	2.120(1)	N2 = N6	2.123	3.1244(2)	226.23	276.35	275.00	b
$[(MeCTp^{3\text{-}i\text{Pr}})Mg(AlMe_4)_2]$ (12)	**6**	**2.211(3)**	**2.200(4)**	**N2 = N6**	**2.207**	**3.276(5)**	**204.31**	**248.78**	**248.76**	**b**
[(dme)(thf)Mg(pz)$_3$MgMe] (**5**)	4	2.078(2)	2.106(2)	2.076(2)	2.087	–	191.09	232.82	232.75	b
$[(HCTp^{Me,Me})_2Mg][OTf]_2$	6	2.172(3) 2.173(3)	2.157(3) 2.162(3)	2.185(3) 2.160(3)	2.170	3.144 3.162	205.43 205.85	249.71 250.54	249.74 250.56	36a
$[(CTp)_2Mg]$	6	2.145(3)	2.195(2)	N4 = N6	2.178	3.249	162.31	201.78	201.89	41
$[(CTp^{Me,Me})_2Mg]$	6	2.189(1)	N2 = N4	N2 = N6	2.189	3.198	204.58	248.43	248.45	36a
$[(CTp^{Me,Me,Me})_2Mg]$	6	2.185(2)	N2 = N4	N2 = N6	2.185	3.215	205.08	249.14	249.14	15
$[(CTp)Mg(CTp^{Me,Me})]$	6	2.186(3) 2.197(3)	2.1609(1) 2.177(2)	N4 = N6 N4 = N6	2.169 2.184	3.267 3.196	161.02 205.15	200.69 248.33	200.68 248.32	14b
$[(CTp^{Ad,Me})MgMe]$	4	2.130(1)	N2 = N4	N2 = N6	2.130	3.046	233.58	283.51	301.47	44
$[(Et_3AlCTp)_2Mg]$	6	2.130(2)	2.150(2)	2.154(2)	2.144	3.264	164.87	205.45	205.46	41
$[(Tp^{Me,Me})MgMe]$	4	2.084(2)	2.084(4)	N2 = N6	2.084	3.071	216.79	264.46	262.21	4
$[(Tp^{3\text{-}t\text{Bu}})MgMe]$	4	2.130(10)	2.137(7)	N4 = N6	2.195	3.068	217.89	265.26	274.25	42
$[(Tp^{t\text{Bu},Me})MgMe]$	4	2.129(1)	N2 = N4	N2 = N6	2.129	3.037	225.48	273.01	273.47	4
$[(PhTp^{3\text{-}t\text{Bu}})MgMe]$	4	2.103(1)	2.148(1)	2.134(1)	2.128	3.132	230.79	279.33	279.40	43
$[(Tp^{Me,Me})Mg(\eta^2\text{-}AlMe_4)]$	5	2.079(2)	2.183(2)	2.089(2)	2.117	3.037	208.73	249.96	252.01	4
$[(Tp^{Me,Me})Mg(\eta^3\text{-}AlMe_4)]$	6	2.115(2)	2.112(2)	2.115(2)	2.114	3.073	208.38	248.85	248.82	4

[a] Θ = directly determined from atomic positions; Θ_{vdw} = consideration of Van der Waals radii; Θ° = mathematical exact. [b] this work.

A general overview of the determined cone angles is summarized in Table 1. Cone angle calculations of $[(Me_3AlCTp^{3\text{-}Me})Mg(AlMe_4)]$ (**8**) (Θ° = 252.46°, CN = 5) compare well with earlier reported $[(Tp^{Me,Me})Mg(AlMe_4)]$ (Θ° = 252.01, CN = 5; Θ° = 248.82, CN = 6). It is noteworthy that the exact cone angle in the latter is significantly affected already by variation of the coordination number 5→6. For metal-in-a-box complexes with CN = 6, a series of Tp/CTp-analogues were considered showing a clear alignment/compliance: **9a** (Θ° = 206.22°)/**9b** (Θ° = 206.70)/$[(CTp)_2Mg]$ (Θ° = 201.89)[41]/$[(Et_3AlCTp)_2Mg]$ (Θ° = 205.46),[41] as well as **9c** (Θ° = 252.42)/**9d** (Θ° = 252.01)/$[(HCTp^{Me,Me})_2Mg][OTf]_2$ (Θ° = 249.74/250.56)[36a]/$[(CTp^{Me,Me})_2Mg]$ (Θ° = 248.45)[36a] /$[(CTp^{Me,Me,Me})_2Mg]$ (Θ° = 249.14).[15] For 3-Ph

substituted ligands it remains challenging to predict a distinct range due to conformational changes of the phenyl rings towards the metal center (**7** (Θ° = 272.87, CN = 6)/**10a** (Θ° = 282.84, CN = 4)). Magnesium complexes with a terminal Mg-Me moiety embedded in *tert*-butyl-substituted polypyrazolyl ligands display an exclusive tetrahedral coordination geometry and hence very similar cone angles (**10b** (Θ° = 275.00) / [(Tp$^{3\text{-}t\text{Bu}}$)MgMe] (Θ° = 274.25)[42]/[(Tp$^{t\text{Bu,Me}}$)MgMe] (Θ° = 273.47)/[(PhTp$^{3\text{-}t\text{Bu}}$)MgMe] (Θ° = 279.40).[43] The most sterically demanding ligand known to date HCTp$^{\text{Ad,Me}}$ adopts an extreme cone angle Θ° = 301.47 in [(CTp$^{\text{Ad,Me}}$)MgMe].[44] An important finding is that the ligand cone angle Θ° = 248.76 for [(MeCTp$^{3\text{-}i\text{Pr}}$)Mg{(μ_2-Me)AlMe$_3$}{(μ_2-Me)$_2$AlMe$_2$}] (**12**, illustrated in Figure 10) is slightly decreased in comparison to supposedly sterically less demanding systems in [(RCTp$^{3\text{-Me}}$)$_2$Mg][AlMe$_4$]$_2$ (**9c**-**d**). However, the intramolecular repulsion of the *i*Pr groups would not allow the formation of a bis-CTp metal-in-a-box complex. Moreover, effects such as coordinating ligands (e.g., donor solvents) and coordination mode of the CTp ligand (κ^3/κ^2) must also be taken into account.

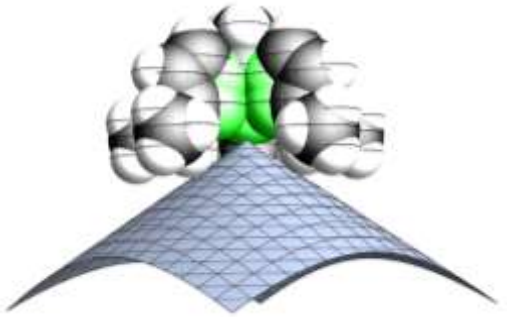

Figure 10. Exact ligand cone angle calculation for MeCTp$^{3\text{-}i\text{Pr}}$ in **12**. The top of the cone represents the center of the metal (see ESI).

Conclusions

Following Elguero's phase transfer catalysis protocol and subsequent electrophilic backbone substitution, the library of tris(pyrazolyl)alkane ligands RCTp$^{3\text{-R'}}$ could be substantially expanded. Depending on the R/R' substitution pattern such potentially tripodal scaffolds exhibit distinct reactivity toward thermally stable homoleptic magnesium tetramethylaluminate Mg(AlMe$_4$)$_2$. Importantly, the substitution at the *C*N3 backbone carbon atom is a crucial factor as the C−H, C−SiMe$_3$, and C−Bn moieties are prone to nucleophilic attack. This is in accord with previous studies on the reactivity of tris(pyrazolyl)alkane ligands with alkylating agents, resulting in deprotonation and methanide formation. We found that introducing alkyl substituents at the *C*N3 backbone carbon atom leads to an overall markedly enhanced stabilization of the RCTp$^{3\text{-R'}}$ ligands, facilitating the synthesis of a variety of magnesium methyl complexes.

Combining Mg(AlMe$_4$)$_2$ with sterically less demanding RCTp$^{3\text{-R'}}$ ligands afforded homoleptic dicationic complexes [(RCTp$^{3\text{-R'}}$)$_2$Mg] with [AlMe$_4$] or [Al$_2$Me$_7$] counterions, the reactivity and structural elucidation of which being reminiscent of solvent-separated ion pairs involving [Mg(do)$_6$]$^{2+}$ cations (e.g., do = thf). Remarkably, the sterically demanding ligands MeCTp$^{3\text{-Ph}}$ and MeCTp$^{3\text{-}t\text{Bu}}$ stabilize the monocationic fragment [MeMg]$^+$ bearing relevance to postmetallocene-based olefin polymerization. Providing the *C*N3 backbone carbon atom with an *n*Bu substituent, that is changing the solubility of the ligand, resulted in the unusual structure of a methyl-bridged dimagnesium species with a rare κ^2-coordinated *n*BuCTp$^{3\text{-Ph}}$ ligand. *i*Propyl-substituted ligand MeCTp$^{3\text{-}i\text{Pr}}$ seems to comply perfectly with any size/sterics criteria, giving access to an intact bis(tetramethyl)aluminate complex, (MeCTp$^{3\text{-}i\text{Pr}}$)$_2$Mg(AlMe$_4$)$_2$, and efficiently counteracting "metal-in-a-box" formation. As detected previously in rare-earth metal chemistry, the [AlMe$_4$] moiety extends to the entire range of coordination modes comprising η^1, η^2, and η^3 as well as η^0 in separated ion pairs.

Why Mg(AlMe$_4$)$_2$? Reactions conducted with [MgMe$_2$]$_n$ are particularly difficult to control resulting in complex mixtures and rapid decomposition of the ligands RCTp$^{3\text{-R'}}$. Hence, the organoaluminum moieties seem to have a stabilizing effect facilitating controlled reactions and the isolation of complexes with intact tris(pyrazolyl)alkane or methanide ligands.

Finally, cone angles Θ have been calculated for the complexes under study and put into perspective with related ones reported in literature. The current work features the determination of cone angles of such potentially tripodal ligands in particular on the premise that it might have a major impact on our understanding of the coordination chemistry and kinetics involved as well as any emerging catalytic properties of the complexes accessed.

Experimental

General Considerations. All manipulations were performed with rigorous exclusion of air and water in an argon-filled glovebox (MBraun MB150B-G; <1 ppm O_2, <1 ppm H_2O) or according to standard Schlenk techniques. Solvents were purified by using Grubbs columns (MBraun SPS-800, solvent purification system) and stored in a glovebox. Acetophenone (>98%), 3-methylbutanone (99%), pinacolone (98%), *n*-butyliodide (99%), chlorotrimethylsilane (99%) benzylbromide (98%), tetra-*n*-butylammonium bromide (98%), diethyleneglycolydimethyl ether (diglyme, >99%), methylmagnesium bromide (3.0 M in Et$_2$O), methylmagnesium chloride (3.0 M in thf), hydrazine hydrate (50-60%) were purchased from Sigma Aldrich and used as received. 1-H-Pyrazole (98%), 3-methyl-1H-pyrazole (99%), iodomethane, methyl *tert*-butyl ether (mtbe) (99%) were purchased from Acros Organics and used as received. Li[N(SiMe$_3$)$_2$] was synthesized according to standard procedures by treatment of the proligand with *n*BuLi. MeCTp, BnCTp,[27] MeCTp$^{3\text{-Me}}$,[45] MeCTp$^{3\text{-Ph}}$,[27] BnCTp$^{3\text{-Ph}}$,[27] MeCTp$^{3\text{-}t\text{Bu}}$,[27] [MgMe$_2$]$_n$ (**4**)[35] Mg(AlMe$_4$)$_2$ (**6**)[29]

were synthesized according to literature procedures. Solvent-free $[MgMe_2]_n$ (**4**) was obtained by de-solvating 1,4-dioxane adduct **4a** under high vacuum (10^{-4} mbar) at 130 °C (**4**) for 24 h. 1,2 difluorobenzene (1,2-DFB) was purchased from Sigma Aldrich, dried over CaH_2, distilled and degassed prior to use. [D_6]benzene, [D_8]toluene and [D_8]thf were purchased from Eurisotop, dried over NaK alloy for two days and filtered prior to use. ^{1}H NMR and ^{13}C{1H} NMR spectra were recorded on a Bruker AVII+400 (^{1}H: 400.13 MHz; ^{13}C 125.76 MHz) spectrometer at 299 K. ^{1}H NMR spectra of **12** were recorded by using a *J. Young* valve NMR tube at variable temperatures on a Bruker AVII+500 instrument (^{1}H: 500.13 MHz; ^{13}C: 125.76 MHz). Infrared spectra were recorded on a Thermo Fisher Scientific NICOLET 6700 FTIR spectrometer using a DRIFT chamber with dry KBr/sample mixtures and KBr windows. DRIFT data were converted using the Kubelka-Munk refinement. CHN elemental analyses were performed on an Elementar vario MICRO cube. EI mass spectra were measured using a Thermo Finnigan TSQ 70.

***n*BuCTp (3b).** $HCTp^{3\text{-}H}$ (3.00 g, 14.9 mmol) was dissolved in 100 mL of thf and cooled to –78 °C. Li[$N(SiMe_3)_2$] (3.05 g, 18.2 mmol) dissolved in 50 mL of thf was added via syringe. The chilled reaction mixture was stirred for another 30 min at ambient temperature and cooled again to –78°C. After dropwise addition of *n*BuI (4.13 g, 22.4 mmol) the reaction was stirred overnight at ambient temperature. Brine solution (50 mL) was added and the aqueous phase was extracted with Et_2O (3x50 mL). The combined organic layers were dried over Na_2SO_4 and filtered. Removing the solvent in vacuo gave **3b** (2.35 g, 8.68 mmol, 62%) as yellow oil. ^{1}H NMR (400.1 MHz, [D_8]toluene, 26 °C): δ = 7.43 (dd, 3H, $^3J_{HH}$ = 1.7 Hz, $^4J_{HH}$ = 0.6 Hz, 3H, 3-*H*(pz)), 6.73 (dd, 3H, $^3J_{HH}$ = 2.6 Hz, $^4J_{HH}$ = 0.7 Hz, 5-*H*(pz)), 5.90 (dd, 3H, $^3J_{HH}$= 2.6 Hz, $^4J_{HH}$ = 1.8 Hz, 4-*H* (pz)), 3.43 (m, 2H, CH_2C$(pz)_3$), 1.75 (m, 2H, CH_2CH_2C$(pz)_3$), 1.27 (sext, 2H, $^3J_{HH}$ = 7.3 Hz, $CH_3CH_2CH_2$), 0.80 (t, 3H, $^3J_{HH}$ = 7.8 Hz, CH_3CH_2) ppm. ^{13}C{^{1}H} NMR (100.6 MHz, [D_8]toluene, 26 °C): δ = 141.0 (3-*C*(pz)), 129.9 (5-*C*(pz)), 106.2 (4-*C*(pz)), 92.8 (*C*$(pz)_3$), 40.8 (*C*H_2C$(pz)_3$), 26.5 (*C*H_2CH_2C$(pz)_3$), 23.1 (CH_3CH_2), 14.1 (*C*H_3CH_2) ppm. IR[Nujol]: $\tilde{\nu}_{max}$ = 3107 (w), 1765 (vw), 1587 (w), 1516 (m), 1421 (m), 1328 (m), 1257 (m), 1238 (m), 1198 (m), 942 (m), 916 (m), 880 (w), 846 (m), 748 (s), 676 (w), 637 (w), 612 (w) cm^{-1}. MS (EI): 270.1, 214.1, 203.2, 173.1, 160.1, 147.1, 135.1, 119.1, 106.1, 93.1, 81.1, 69.1.

***n*BuCTp$^{3\text{-}Me}$ (3e).** Following the procedure described for **3b**, $HCTp^{3\text{-}Me}$ (5.00 g, 19.5 mmol), *n*BuLi (8.59 mL, 21.5 mmol, 2.5 M in *n*-hexane) and *n*BuI (2.44 mL, 21.5 mmol) yielded a yellow solid as crude product. Further purification was achieved by recrystallization from mtbe generating **3e** as colorless crystals (1.44 g, 4.60 mmol, 24%) suitable for X-ray diffraction analysis. ^{1}H NMR (400.1 MHz, $CDCl_3$, 26 °C): δ = 6.80 (dd, 3H, $^3J_{HH}$ = 2.5 Hz, $^4J_{HH}$ = 0.5 Hz, *5*-H(pz)), 6.03 (dd, 3H, $^3J_{HH}$ = 2.6 Hz, $^4J_{HH}$ = 0.4 Hz, *4*-H(pz)), 3.18 (m, 2H, CH_2C$(pz)_3$), 2.28 (s, 9H, (pz)-CH_3), 1.55 (m, 2H, CH_2CH_2C$(pz)_3$), 1.38 (sex, 2H, $^3J_{HH}$ = 7.5 Hz, $CH_3CH_2CH_2$), 0.90 (t, 3H, $^3J_{HH}$ = 7.3 Hz, CH_3CH_2) ppm. ^{13}C{^{1}H} NMR (100.6 MHz, $CDCl_3$, 26 °C): δ = 150.5 (3-*C*(pz)), 130.7 (5-*C*(pz)), 106.2 (4-*C*(pz)), 91.6 (*C*$(pz)_3$), 40.2 (*C*H_2C$(pz)_3$), 26.1 (*C*H_2CH_2C$(pz)_3$), 22.9 (CH_3CH_2), 14.1 (*C*H_3CH_2), 14.0 ((pz)-*C*H_3) ppm. DRIFT: $\tilde{\nu}_{max}$ = 3138 (vw), 3114 (w), 2987 (w), 2952 (s), 2928 (m), 2868 (m), 2965 (m), 1721 (vw), 1711 (vw), 1621 (vw), 1530 (vs), 1460 (s), 1453 (s), 1391 (s), 1372 (m), 1354 (s), 1341 (m), 1209 (vs), 1198 (vs), 1132 (vw), 1118 (vw), 1062 (s), 963 (w), 934 (m), 907 (m), 844 (vs), 765 (vs), 723 (vw), 680 (m), 650 (w), 618 (vw) cm^{-1}. $C_{17}H_{24}N_6$ (312.4 g·mol^{-1}) calcd. C 65.36, H 7.74, N 26.90; found C 65.43, H 7.96, N 27.01.

Me$_3$SiCTp$^{3\text{-}Me}$ (3f). Following the procedure described above for **3b**, $HCTp^{3\text{-}Me}$ (5.00 g, 19.5 mmol), *n*BuLi (8.59 mL, 21.5 mmol, 2.5 M in *n*-hexane) and Me_3SiCl (4.1 mL, 32.2 mmol) yielded a yellow solid as crude product. Further purification was achieved by recrystallization from mtbe and gave **3f** as colorless crystals (4.05 g, 12.3 mmol, 63%) suitable for X-ray diffraction analysis. ^{1}H NMR (400.1 MHz, $CDCl_3$, 26 °C): δ = 6.57 (d, 3H, $^3J_{HH}$ = 2.4 Hz, 5-*H*(pz)), 6.03 (d, 3H, $^3J_{HH}$ = 2.5 Hz, 4-*H*(pz)), 2.28 (s, 9H, (pz)-CH_3), 0.28 (s, 9H, Si(CH_3)$_3$) ppm. ^{13}C{^{1}H} NMR (100.6 MHz, $CDCl_3$, 26 °C): δ = 150.1 (3-*C*(pz)), 129.4 (5-*C*(pz)), 105.8 (4-*C*(pz)), 89.4 (*C*$(pz)_3$), 14.0 ((pz)-*C*H_3), –0.59 (Si(*C*H_3)$_3$) ppm. DRIFT: $\tilde{\nu}_{max}$ = 3134 (m), 3119 (m), 2982 (m), 2955 (m), 2928 (m), 2899 (m), 1608 (w), 1525 (vs), 1449 (s), 1391 (s), 1356 (vs), 1243 (vs), 1203 (vs), 1058 (vs), 997 (m), 936 (w), 921 (w), 837 (vs), 788 (vs), 758 (vs), 700 (m), 675 (m), 660 (m), 632.78 (s), 619 (w) cm^{-1}. $C_{16}H_{24}N_6Si$ (328.5 g·mol^{-1}) calcd. C 58.50, H 7.36, N 25.58; found C 58.11, H 6.80, N 25.83.

***n*BuCTp$^{3\text{-}Ph}$ (3h).** Following the procedure described for **3b**, $HCTp^{3\text{-}Ph}$ (3.30 g, 7.46 mmol), Li[$N(SiMe_3)_2$] (1.62 g, 9.69 mmol) and *n*-BuI (1.50 mL, 11.2 mmol) yielded a yellow solid as crude product. Further purification was achieved by recrystallization from Et_2O yielding **3h** as colorless crystals (1.95 g, 3.91 mmol, 52%) suitable for X-ray structure analysis. ^{1}H NMR (400.1 MHz, $CDCl_3$, 26 °C): δ = 7.86 (m, 6H, *o*-*H*(Ph)), 7.38 (m, 9H, *m*-*H*(Ph), *p*-*H*(Ph)), 7.07 (d, 3H, $^3J_{HH}$ = 2.7 Hz, 5-*H*(pz)), 6.62 (d, 3H, $^3J_{HH}$ = 2.7 Hz, 4-*H*(pz)), 3.49 (m, 2H, CH_2C$(pz)_3$), 1.83 (m, 2H, CH_2CH_2C$(pz)_3$), 1.50 (sext, 2H, $^3J_{HH}$ = 7.6 Hz, $CH_3CH_2CH_2$), 1.00 (t, 3H, $^3J_{HH}$ = 7.4 Hz, CH_3CH_2) ppm. ^{13}C{^{1}H} NMR (100.6 MHz, $CDCl_3$, 26 °C): δ = 153.1 (3-*C*(pz)), 133.1 (1-*C*(Ph)), 131.5 (5-*C*(pz)), 128.8 (o-*C*(Ph)), 128.3 (*p*-*C*(Ph)), 126.1 (*m*-*C*(Ph)), 103.6 (4-*C*(pz)), 92.9 (*C*$(pz)_3$), 40.1 (*C*H_2C$(pz)_3$), 26.3 (*C*H_2CH_2C$(pz)_3$), 23.0 (CH_3CH_2), 14.1 (*C*H_3CH_2) ppm. DRIFT: $\tilde{\nu}_{max}$ = 3145 (vw), 3118 (w), 3087 (vw), 3061 (vw), 3035 (vw), 2953 (w), 2978 (w), 2870 (vw), 1974 (vw), 1954 (vw), 1887 (vw), 1808 (vw), 1762 (vw), 1700 (vw), 1604 (vw), 1528 (w), 1498 (m), 1456 (s), 1385 (m), 1358 (m), 1271 (m), 1238 (m), 1213 (s), 1099 (w), 1074 (m), 1047 (m), 842 (m), 751 (s), 694 (s), 662 (w) cm^{-1}. $C_{32}H_{30}N_6$ (498.4 g·mol^{-1}) calcd. C 77.08, H 6.06, N 16.85; found C 77.22, H 6.15, N 16.04.

MeCTp$^{3\text{-}iPr}$ (3j). Following the procedure described for **3b**, HCTp$^{3\text{-}iPr}$ (8.91 g, 26.2 mmol), Li[N(SiMe$_3$)$_2$] (5.69 g, 34.0 mmol) and MeI (2.44 mL, 39.3 mmol) yielded a dark brown solid as crude product. Further purification was achieved by recrystallization from mtbe generating **3j** as colorless crystals (2.36 g, 6.65 mmol, 25%) suitable for X-ray diffraction analysis. ^{1}H NMR (400.1 MHz, CDCl$_3$, 26°C): δ = 6.42 (d, 3H, $^3J_{HH}$ = 2.6 Hz, 5-*H*(pz)), 6.07 (d, 3H, $^3J_{HH}$ = 2.7 Hz, 4-*H*(pz)), 3.00 (sept, 3H, $^3J_{HH}$ = 7.1 Hz, (CH$_3$)$_2$C*H*(pz)), 2.90 (s, 3H, C*H*$_3$C(pz)$_3$), 1.24 (d, 18H, $^3J_{HH}$ = 7.0 Hz, (C*H*$_3$)$_2$CH(pz)) ppm. ^{13}C{^{1}H} NMR (100.6 MHz, CDCl$_3$, 26 °C): δ = 161.3 (3-*C*(pz)), 129.6 (5-*C*(pz)), 103.3 (4-*C*(pz)), 90.4 (*C*(pz)$_3$), 28.13 ((CH$_3$)$_2$CH(pz)), 25.8 (*C*H$_3$C(pz)$_3$), 23.0 ((CH$_3$)$_2$CH(pz)) ppm. DRIFT: $\tilde{\nu}_{max}$ = 3138 (vw), 3120 (vw), 2963 (vs), 2927 (m), 2869 (m), 1608 (vw), 1524 (s), 1470 (w), 1449 (m), 1386 (m), 1370 (s), 1298 (m), 1258 (vs), 1217 (vs), 1156 (vw), 1113 (w), 1049 (m), 985 (m), 975 (m), 924 (vw), 881 (vw), 792 (vs), 769 (vs), 721 (w), 641 (vw), 577 (vw) cm^{-1}. C$_{20}$H$_{30}$N$_6$ (498.4 g·mol^{-1}) calcd. C 67.76, H 8.53, N 23.71; found C 67.63, H 7.92, N 23.87.

[MgMe$_2$(dioxane)]$_n$ (4a). Solid [MgMe$_2$]$_n$ (100 mg, 1.85 mmol) was dissolved in 2 mL of 1,4-dioxane, sealed in a scintillation vial and stored inside a glovebox at ambient temperature. After several months the solution contained colorless crystals of **4a** suitable for single-crystal structure analysis. Since **4a** is insoluble in [D$_6$]benzene the ^{1}H NMR spectrum was recorded in [D$_8$]thf indicating dimeric [MgMe(□$_2$-Me)(thf)]$_2$. C$_{16}$H$_{14}$MgO$_2$ (142.48 g mol^{-1}) calcd. C 50.58, H 9.90; found C 50.40, H 9.85. Further analytical data are found in literature.[18a]

[MgMe$_2$(diglyme)] (4b). To a stirred solution of [MeMgCl(thf)$_2$] (70.0 mg, 320 μmol) in 5 mL of toluene diglyme (21.4 mg, 160 μmol) was added. A white precipitate of MgCl$_2$(diglyme) formed immediately. After 30 min the mixture was centrifuged and the solid residue was extracted with 3x3 mL toluene. To the filtrate 0.5 mL diglyme was added and excess toluene was removed under reduced pressure. Colorless crystals of **4b** were obtained from a saturated diglyme solution at –40 °C (25.2 mg, 84%). The ^{1}H NMR spectrum revealed adduct formation [MgMe$_2$(diglyme)]·1.5diglyme. ^{1}H NMR ((400.1 MHz, [D$_6$]benzene, 26 °C): δ = 3.17 (s, 4H, H$_3$C–O–CH$_2$C*H*$_2$), 3.12 (s, 4H, H$_3$C–O–C*H*$_2$CH$_2$), 3.12 (s, 6H, *H*$_3$C–O–CH$_2$CH$_2$), –0.91 (s, 2.34H, MgC*H*$_3$) ppm. Further analytical data are found in the literature.[46]

[(dme)(thf)Mg(pz)$_3$MgMe] (5). To a suspension of [MgMe$_2$]$_n$ (**4**) (50.0 mg, 920 μmol, evaporated to dryness under high vacuum) in 1.5 mL of toluene a solution of BnCTp (280 mg, 920 μmol) dissolved in 1.5 mL of toluene was added dropwise. The solution cleared up and turned immediately yellow. After addition of a 1:1 mixture dme/thf (2 mL) and stirring for 30 s, the reaction mixture was stored at –40 °C. Some brown single crystals of **5** as decomposition product suitable for X-ray diffraction analysis were collected. Due to ongoing rapid decomposition, further characterization was not successful.

(Me$_3$AlCTp$^{3\text{-}Ph}$)$_2$Mg (7). To a suspension of HCTp$^{3\text{-}Ph}$ (134 mg, 302 μmol) in 2 mL of toluene a solution of **6** (60.0 mg, 302 μmol) in 2 mL of *n*-hexane was added dropwise. The reaction cleared up and was stirred for 2 h at ambient temperature. After removing the solvent under reduced pressure, the crude product was recrystallized in *n*-hexane at ambient temperature producing colorless crystals of **7** suitable for X-ray diffraction analysis. A better elemental analysis could not be obtained due to residual *n*-hexane and toluene (141 mg, 134 μmol, 89%). ^{1}H NMR (400.1 MHz, [D$_6$]benzene, 26 °C): δ = 8.90 (d, 6H, $^3J_{HH}$ = 2.8 Hz, 5-*H*(pz)), 6.70 (m, 18H, *o*-*H*(Ph)/*p*-*H*(Ph)), 6.54 (m, 12H, *m*-*H*(Ph)), 5.68 (d, 6H, $^3J_{HH}$ = 2.8 Hz, 4-*H*(pz)), 0.26 (s, 18H, Al(C*H*$_3$)$_3$) ppm. ^{13}C{^{1}H} NMR (100.6 MHz, [D$_6$]benzene, 26 °C): δ = 156.4 (3-*C*(pz)), 138.6 (5-*C*(pz)), 131.1 (1-*C*(Ph)), 128.4 (*o*-*C*(Ph)), 128.0 (*p*-*C*(Ph)), 127.3 (*m*-*C*(Ph)), 105.93 (4-*C*(pz)), 87.5 (*C*(pz)$_3$), –2.2 (Al(*C*H$_3$)$_3$) ppm. DRIFT: $\tilde{\nu}_{max}$ = 3157 (vw), 3137 (vw), 3027 (vw), 2923 (w), 2887 (w), 2820 (vw), 1603 (vw), 1531 (w), 1496 (vw), 1470 (w), 1447 (w), 1404 (w), 1404 (w), 1380 (w), 1249 (vw), 1226 (vw), 1182 (m), 1110 (vw), 1071 (m), 1057 (m), 1028 (vw), 1001 (vw), 952 (vw), 918 (vw), 810 (m), 779 (m), 759 (s), 709 (vs), 644 (m), 619 (w), 579 (w) cm^{-1}. C$_{62}$H$_{62}$MgAl$_2$N$_{12}$ (1053.53 g·mol^{-1}) calcd. C 70.68, H 5.93, N 15.95; found C 71.32, H 5.80, N 15.01.

(Me$_3$AlCTp$^{3\text{-}Me}$)Mg(AlMe$_4$) (8). Following the procedure described for **7**, **6** (70.0 mg, 353 μmol) and Me$_3$SiCTp$^{3\text{-}Me}$ (116 mg, 353 μmol) yielded **8** as a white powder in almost quantitative yield (149 mg, 340 μmol, 96%). Colorless crystals of **8** were grown from saturated 1:1 *n*-hexane/toluene mixture at –40 °C. ^{1}H NMR (400.1 MHz, [D$_6$]benzene, 26 °C): δ = 8.49 (d, 3H, $^3J_{HH}$ = 2.6 Hz, 5-*H*(pz)), 5.31 (d, 3H, $^3J_{HH}$ = 2.5 Hz, 4-*H*(pz)), 1.82 (s, 9H, (pz)-C*H*$_3$), 0.03 (s, 9H, Al(C*H*$_3$)$_3$), –0.19 (s, 12H, [Al(C*H*$_3$)$_4$]) ppm. ^{13}C{^{1}H} NMR (100.6 MHz, CDCl$_3$, 26 °C): δ = 151.4 (3-*C*(pz)), 137.4 (5-*C*(pz)), 105.6 (4-*C*(pz)), 84.9 (*C*(pz)$_3$), 13.7 ((pz)-*C*H$_3$), –3.6 (Al(*C*H$_3$)$_3$), –5.13 ([Al(*C*H$_3$)$_4$]) ppm. DRIFT: $\tilde{\nu}_{max}$ = 3156 (vw), 2925 (w), 2890 (vw), 1525 (w), 1495 (vw), 1414 (vw), 1389 (vw), 1369 (w), 1227 (vw), 1181 (m), 1063 (s), 1040 (vw), 1002 (vw), 810 (s), 770 (s), 723 (vs), 712 (vs), 677 (m), 655 (w), 638 (w), 608 (vw), 570 (vw), 532 (w) cm^{-1}. C$_{20}$H$_{36}$MgAl$_2$N$_6$ (438.82 g·mol^{-1}) calcd. C 54.74, H 8.27, N 19.15; found C 54.38, H 8.04, N 18.49.

[(MeCTp$^{3\text{-}H}$)$_2$Mg][AlMe$_4$]$_2$ (9a). To a solution of **6** (52.3 mg, 263 μmol) in 2 mL of *n*-hexane a solution of MeCTp (120 mg, 526 μmol) in 2 mL of toluene was added dropwise. A white precipitate formed immediately. After stirring overnight at ambient temperature, the reaction mixture was dried under reduced pressure. The crude product was washed with *n*-pentane (3x5 mL) affording **9a** as white powder in almost quantitative yield (168 mg, 257 μmol, 97%). Colorless crystals of **9a** were grown by diluting 50 mg product in 1 mL of thf and evaporation of the solvent in vacuo. The resulting brownish oil crystallized at

ambient temperature. The NMR sample contained a mixture of complex **9a** (species a), free ligand and mono-ligand species b in 1:3:1 ratio. ^{1}H NMR (400.1 MHz, [D$_8$]thf, 26 °C): δ = 8.59 (d, 3H, $^{3}J_{HH}$ = 2.9 Hz, 5-*H*(pz), free ligand), 8.51 (s, 1.2 H, 5-*H*(pz), species a), 8.01 (s, 1.2H, 3-*H*(pz), species a), 7.65 (d, 3H, $^{3}J_{HH}$ = 2.1 Hz, 3-*H*(pz), free ligand), 7.56 (s, 1.1H, 5-*H*(pz), species b), 6.76 (s, 1.1 H, 3-*H*(pz), species b), 6.64 (s, 1.2H, 4-*H*(pz), species a), 6.60 (t, 3H, $^{3}J_{HH}$ = 2.4 Hz, 4-*H*(pz), free ligand), 6.26 (s, 1.1H, 4-*H*(pz), species b), 3.52 (s, 3H, C*H*$_3$C(pz)$_3$, free ligand), 3.44 (s, 3H, C*H*$_3$C(pz)$_3$, species a), 3.52 (s, 3H, C*H*$_3$C(pz)$_3$, species b), –1.34 (m, 24H, [Al(C*H*$_3$)$_4$]) ppm. ^{13}C{^{1}H} NMR (100.6 MHz, [D$_8$]thf, 26 °C): (100.6 MHz, CDCl$_3$, 26 °C): δ = 144.3/141.7 (3-*C*(pz)), 133.4/129.8 (5-*C*(pz)), 108.6/108.4 (4-*C*(pz)), 85.1 (*C*(pz)$_3$), 23.7/23.4 (*C*H$_3$C(pz)$_3$), – 4.5 (sext, $^{1}J_{C\text{-}Al}$ = 74.9 Hz, [Al(*C*H$_3$)$_4$]) ppm. DRIFT: $\tilde{\nu}_{max}$ = 3158 (w), 3142 (w), 3111 (vw), 2904 (m), 2800 (w), 1523 (vw), 1416 (m), 1389 (w), 1322 (s), 1233 (s), 1218 (vw), 1207 (vw), 1134 (m), 1123 (m), 1090 (m), 1065 (s), 977 (m), 921 (vw), 862 (vw), 775 (vs), 764 (vs), 734 (w), 694 (s), 603 (m), 590 (w), 546 (m) cm^{-1}. $C_{30}H_{48}MgAl_2N_{12}$ (655.07 g·mol^{-1}) calcd. C 55.01, H 7.39, N 25.66; found C 55.46, H 7.44, N 23.75.

[(*n*BuCTp$^{3\text{-}H}$)$_2$Mg][AlMe$_4$]$_2$ (9b). Following the procedure described for **9a**, **6** (50.0 mg, 252 μmol) and *n*BuCTp (136 mg, 504 μmol) yielded **9b** as a white powder (168 mg, 227 μmol, 90%). Colorless crystals were grown analogously to **9a**. For compound **9b** a concentration-dependent decomposition in solution was observed. In order to counteract degradation the NMR spectra of **9b** were recorded as highly diluted, 25 μmolar solutions. When increasing the concentration to record the ^{13}C NMR spectrum the sample started to decompose and distinct ligand species were detected. ^{1}H NMR (400.1 MHz, [D$_8$]thf, 26 °C): δ = 7.60 (s, 4H, 5-*H*(pz)), 7.04 (s, 4H, 3-*H*(pz)), 6.29 (s, 4H, 4-*H*(pz)), 3.29 (m, 4H, C*H*$_2$C(pz)$_3$), 1.59 (m, 4H, C*H*$_2$CH$_2$C(pz)$_3$), 1.39 (sext, 4H, $^{3}J_{HH}$ = 7.2 Hz, CH$_3$C*H*$_2$CH$_2$), 0.89 (t, 6H, $^{3}J_{HH}$ = 7.4 Hz, C*H*$_3$CH$_2$), −0.96 (s), −1.30 (s), −1.67 (s) (24H, Al(C*H*$_3$)$_3$(thf), [Al(C*H*$_3$)$_4$], [*n*BuCTpMg(C*H*$_3$)(thf)$_2$]) ppm. ^{13}C{^{1}H} NMR (100.6 MHz, [D$_8$]thf, 26 °C): (100.6 MHz, CDCl$_3$, 26 °C): δ = 144.2 (3-*C*(pz)), 141.4 (3-*C*(pz), free ligand), 134.3 (5-*C*(pz)), 130.6 (5-*C*(pz), free ligand), 109.1 (4-*C*(pz)), 106.6 (4-*C*(pz), free ligand), 92.4 (*C*(pz)$_3$, free ligand), 87.2 (*C*(pz)$_3$), 40.3 (*C*H$_2$C(pz)$_3$), 34.5 (*C*H$_2$C(pz)$_3$, free ligand), 28.1 (*C*H$_2$CH$_2$C(pz)$_3$, free ligand), 27.9 (*C*H$_2$CH$_2$C(pz)$_3$), 26.8 (CH$_3$*C*H$_2$), 23.4 (CH$_3$*C*H$_2$, free ligand), 14.1 (*C*H$_3$CH$_2$, free ligand), –4.7 (sext, $^{1}J_{C\text{-}Al}$ = 70.2 Hz, [Al(*C*H$_3$)$_4$]) ppm. DRIFT: $\tilde{\nu}_{max}$ = 3161 (vw), 3140 (w), 3111 (vw), 2959 (w), 2898 (m), 2800 (w), 1520 (vw), 1414 (m), 1336 (m), 1221 (m), 1198 (w), 1157 (w), 1099 (s), 1069 (s), 956 (m), 923 (vw), 837 (s), 782 (m), 760 (vs), 689 (vs), 639 (m), 539 (m) cm^{-1}. $C_{38}H_{60}MgAl_2N_{12}$ (739.23 g·mol^{-1}) calcd. C 58.49, H 8.18, N 22.74; found C 58.36, H 7.43, N 21.38.

[(MeCTp$^{3\text{-}Me}$)$_2$Mg][AlMe$_4$]$_2$·C$_7$H$_8$ (9c). Following the procedure described for **9a**, **6** (14.8 mg, 74.3 μmol) and MeCTp$^{3\text{-}Me}$ (40.0 mg, 148 μmol) yielded **9c** as a white powder in high yields (51.2 mg, 61.6 μmol, 83%). Colorless crystals of **9c** were grown by dissolving 25 mg product **9c** in 1 mL of diglyme and subsequent slow diffusion of *n*-pentane at ambient temperature. ^{1}H NMR (400.1 MHz, [D$_8$]thf, 26 °C): δ = 8.53 (d, 6H, $^{3}J_{HH}$ = 2.9 Hz, 5-*H*(pz)), 6.48 (s, 6H, $^{3}J_{HH}$ = 2.6 Hz, 4-*H*(pz)), 3.51 (s, 6H, C*H*$_3$C(pz)$_3$, overlapped by diglyme), 1.71 (s, 18H, (pz)-C*H*$_3$), −1.30 (m, 24H, [Al(C*H*$_3$)$_4$]) ppm. ^{13}C{^{1}H} NMR (100.6 MHz, [D$_8$]thf, 26 °C): δ = 155.3 (3-*C*(pz)), 134.1 (5-*C*(pz)), 108.6 (4-*C*(pz)), 84.5 (*C*(pz)$_3$), 24.0 (*C*H$_3$C(pz)$_3$), 12.5 ((pz)-*C*H$_3$), –4.6 (sext, $^{1}J_{C\text{-}Al}$ = 73.1 Hz, [Al(*C*H$_3$)$_4$]) ppm. DRIFT: $\tilde{\nu}_{max}$ = 3160 (vw), 3130 (vw), 3017 (vw), 2902 (m), 2800 (w), 1534 (m), 1482 (w), 1446 (vw), 1416 (vw), 1392 (m), 1374 (m), 1352 (m), 1300 (vw), 1214 (vs), 1154 (w), 1075 (s), 1036 (w), 990 (vw), 777 (vs), 757 (m), 741 (m), 696 (vs), 688 (vs), 662 (m), 615 (w), 576 (vw), 541 (m) cm^{-1}. $C_{36}H_{60}MgAl_2N_{12}$·C_7H_8 (831.37 g·mol^{-1}) calcd. C 62.12, H 8.24, N 20.22; found C 61.69, H 8.23, N 19.70.

[(*n*BuCTp$^{3\text{-}Me}$)$_2$Mg][AlMe$_4$]$_2$ (9d). Following the procedure described for **9a**, **6** (38.1 mg, 192 μmol) and *n*BuCTp$^{3\text{-}Me}$ (120 mg, 384 μmol) yielded **9d** as white powder in quantitative yield (157 mg, 191 μmol, 99%). Colorless crystals of **9d** were grown by heating a solution of **6** (5.00 mg, 25.2 μmol) and *n*BuCTp$^{3\text{-}Me}$ (7.87 mg, 25.2 μmol) in 0.7 mL [D$_6$]benzene in a *J. Young valve* NMR tube to 90 °C for 1 h. ^{1}H NMR (400.1 MHz, [D$_8$]thf, 26 °C): δ = 8.43 (s, 6H, 5-*H*(pz)), 6.56/6.38 (s, 6H, 4-*H*(pz)), 3.85 (m, 4H, C*H*$_2$C(pz)$_3$), 2.16/1.58/1.34 (s, 18H, (pz)-C*H*$_3$), 2.03 (m, 4H, C*H*$_2$CH$_2$C(pz)$_3$), 1.89 (sext, 4H, $^{3}J_{HH}$ = 7.3 Hz, CH$_3$C*H*$_2$CH$_2$), 1.14 (t, 6H, $^{3}J_{HH}$ = 7.3 Hz, C*H*$_3$CH$_2$), –1.30 (m, 24H, [Al(C*H*$_3$)$_4$]) ppm. ^{13}C{^{1}H} NMR (100.6 MHz, [D$_8$]thf, 26 °C): δ = 155.5 (3-*C*(pz)), 150.2 (3-*C*(pz), free ligand), 135.6/132.5 (5-*C*(pz)), 131.2 (5-*C*(pz), free ligand), 109.6/108.9 (4-*C*(pz)), 106.0 (4-*C*(pz), free ligand), 87.3 (*C*(pz)$_3$, free ligand), 40.6 (*C*H$_2$C(pz)$_3$), 35.0 (*C*H$_2$C(pz)$_3$, free ligand), 28.1 (*C*H$_2$CH$_2$C(pz)$_3$, free ligand), 26.7 (*C*H$_2$CH$_2$C(pz)$_3$), 23.5 (CH$_3$*C*H$_2$, free ligand), 14.1 ((pz)-*C*H$_3$, free ligand), 13.6 (*C*H$_3$CH$_2$, free ligand), 13.0 (*C*H$_3$CH$_2$), 12.6 (((pz)-*C*H$_3$), –4.6 (sext, $^{1}J_{C\text{-}Al}$ = 72.5 Hz, [Al(*C*H$_3$)$_4$]) ppm. DRIFT: $\tilde{\nu}_{max}$ = 3159 (vw), 3137 (vw), 2964 (vw), 2899 (m), 2970 (w), 2797 (w), 1532 (m), 1481 (w), 1481 (vw), 1445 (vw), 1408 (vw), 1392 (w), 1381 (w), 1353 (vw), 1288 (vw), 1252 (vw), 1223 (vw), 1190 (m), 1145 (m), 1075 (s), 1035 (w), 978 (vw), 953 (vw), 887 (vw), 836 (w), 820 (w), 776 (s), 693 (vs), 622 (vw), 552 (m) cm^{-1}. $C_{36}H_{60}MgAl_2N_{12}$·C_7H_8 (823.39 g·mol^{-1}) calcd. C 61.27, H 8.81, N 20.41; found C 60.93, H 8.74, N 20.24.

[(MeCTp$^{3\text{-}Ph}$)MgMe][AlMe$_4$] (10a). To a solution of MeCTp$^{3\text{-}Ph}$ (150 mg, 329 μmol) in 2 mL of toluene a solution of **6** (65.2 mg, 329 μmol) in 2 mL of *n*-hexane was added dropwise. Instant formation of a white precipitate was observed. After removing the solvent under reduced pressure, the crude product was washed with *n*-pentane (3x3 mL) yielding **10a** as a white powder (123 mg, 211 μmol, 64%). Colorless crystals of **10a** suitable for X-ray diffraction analysis were grown from a hot toluene solution by cooling to ambient temperature. ^{1}H NMR (400.1 MHz,

[D$_6$]benzene/1,2-DFB, 26 °C): δ = 7.95 (d, 3H, $^3J_{HH}$ = 2.5 Hz, 5-*H*(pz)), 7.26 (m, 6H, *m*-*H*(Ph)), 7.06 (m, 9H, *o*-*H*(Ph)/*p*-*H*(Ph)), 6.13 (d, 3H, $^3J_{HH}$ = 2.7 Hz, 4-*H*(pz)), 3.24 (s, 3H, CH_3C(pz)$_3$), –0.03 (s, 12H, [Al(CH_3)$_4$]), –1.16 (s, 3H, Mg-CH_3) ppm. ^{13}C{^{1}H} NMR (100.6 MHz, [D$_6$]benzene/1,2-DFB, 26 °C): δ = 158.3 (3-*C*(pz)), 133.7 (1-*C*(Ph)), 130.8 (5-*C*(pz)), 129.2 (o-*C*(Ph)), 128.2 (p-*C*(Ph)), 127.9 (m-*C*(Ph)), 107.1 (4-*C*(pz)), 84.7 (*C*(pz)$_3$), 25.2 (*C*H$_3$C(pz)$_3$), –3.1 (Mg-*C*H$_3$/[Al(*C*H$_3$)$_4$], very weak) ppm. DRIFT: $\tilde{\nu}_{max}$ = 3162 (vw), 3144 (vw), 3060 (vw), 3030 (vw), 2905 (m), 2846 (w), 2846 (vw), 2800 (w), 1604 (vw) 1582 (vw), 1534 (m), 1501 (m), 1465 (m), 1384 (m), 1359 (w), 1304 (vw), 1216 (m), 1148 (w), 1118 (w), 1077 (m), 1065 (m), 1028 (vw), 945 (vw), 917 (vw), 772 (s), 756 (s), 695 (vs), 542 (m) cm^{-1}. $C_{34}H_{39}MgAl_2N_6$ (583.01 g·mol^{-1}) calcd. C 70.05, H 6.74, N 14.42; found C 70.20, H 6.18, N 13.76.

[(MeCTp$^{3\text{-}t\text{Bu}}$)MgMe][Al$_2$Me$_7$] (10b). Following the procedure described for **10a**, **6** (100 mg, 504 μmol) and MeCTp$^{3\text{-}t\text{Bu}}$ (200 mg, 504 μmol) yielded **10b** as a white powder in high yields (274 mg, 470 μmol, 91%). Colorless crystals of **10b** suitable for X-ray diffraction analysis were grown from a toluene/1,2-difluorobenzene solution. ^{1}H NMR (400.1 MHz, [D$_6$]benzene/1,2-DFB, 26 °C): δ = 7.45 (d, 3H, $^3J_{HH}$ = 3.0 Hz, 5-*H*(pz)), 5.88 (d, 3H, $^3J_{HH}$ = 2.8 Hz, *4*-H(pz)), 2.72 (s, 3H, C*H*$_3$C(pz)$_3$), 1.20 (d, 27 H, C(C*H*$_3$)$_3$), –0.22 (s, 21H, [Al$_2$(C*H*$_3$)$_7$]), –0.35 (s, 3H, Mg-C*H*$_3$) ppm. ^{13}C{^{1}H} NMR (100.6 MHz, [D$_6$]benzene/1,2-DFB, 26 °C): δ = 168.9 (3-*C*(pz)), 131.6 (5-*C*(pz)), 105.3 (4-*C*(pz)), 83.4 (*C*(pz)$_3$), 32.3 (*C*(CH$_3$)$_3$), 30.2 (C(*C*H$_3$)$_3$), 25.4 (*C*H$_3$C(pz)$_3$), –4.1 (Mg*C*H$_3$), –4.4 ([Al$_2$(CH$_3$)$_7$]) ppm. DRIFT: $\tilde{\nu}_{max}$ =3166 (w), 3149 (w), 2964 (m), 2917 (s), 2876 (w), 2805 (w), 1746 (vw), 1525 (m), 1485 (w), 1462 (w), 1382 (w), 1366 (s), 1304 (vw), 1264 (w), 1221 (s), 1169 (m), 1126 (w), 1079 (s), 1028 (w), 1016 (m), 965 (w), 932 (w), 874 (vw), 771 (vs), 700 (vs), 633 (s), 608 (s), 559 (s), 538 (s), 510 (m) cm^{-1}. $C_{31}H_{60}MgAl_2N_6$ (593.13 g·mol^{-1}) calcd. C 62.56, H 10.16, N 14.12; found C 61.93, H 9.98, N 14.79.

[(BnCTp$^{3\text{-}Ph}$)MgMe][AlMe$_4$]. A solution of BnCTp$^{3\text{-}Ph}$ (15.3 mg, 28.8 μmol) in 0.3 mL of [D$_6$]benzene was added to a solution of **6** (5.72 mg, 28.8 μmol) in a *J. Young* valve NMR tube. The ^{1}H NMR spectra indicated the coordination of the ligand to magnesium, but further attempts to isolate any discrete species failed.

[{(κ^2-(N,N')*n*BuCTp$^{3\text{-}Ph}$)Mg(AlMe$_4$)}$_2$(μ^2-Me)][AlMe$_4$] (11). Following the procedure described for **10a**, **6** (70.0 mg, 353 μmol) and *n*BuCTp$^{3\text{-}Ph}$ (176 mg, 353 μmol) yielded **11** as a white powder in quantitative yield (226 mg, 171 μmol, 97%). Single crystals grown from a hot toluene solution showed a highly disordered lattice toluene and indicated the formation of [Al$_2$Me$_7$] as a counter ion. Colorless crystals of **11** suitable for an accurate X-ray diffraction analysis were grown from a [D$_6$]benzene solution in a *J. Young* valve NMR tube at ambient temperature. ^{1}H NMR (400.1 MHz, [D$_6$]benzene/1,2-DFB 26 °C): δ = 7.81 (s, 6H, 5-*H*(pz)), 7.53 (m, 6H, *m*-*H*(Ph)), 7.21 (m, 24H, *o*-*H*(Ph)/*p*-*H*(Ph)), 6.34 (s, 6H, 4-*H*(pz)), 3.58/2.95 (m, 4H, C*H*$_2$C(pz)$_3$), 1.39 (m, 4H, CH$_3$C*H*$_2$CH$_2$), 1.01 (s, 4H, C*H*$_2$CH$_2$C(pz)$_3$), 0.86 (t, 6H, $^3J_{HH}$ = 7.2 Hz, C*H*$_3$CH$_2$), –0.57 (s, 39H, 13xC*H*$_3$: [Al(C*H*$_3$)$_4$], Mg-C*H*$_3$-Mg, 2x Mg-C*H*$_3$-Al, 2x Al(C*H*$_3$)$_3$) ppm. ^{13}C{^{1}H} NMR (100.6 MHz, [D$_6$]benzene /1,2-DFB, 26 °C): δ = 158.5 (3-*C*(pz)), 134.5 (1-*C*(Ph)), 131.2 (5-*C*(pz)), 129.8 (*o*-*C*(Ph)), 126.0 (m-*C*(Ph)), 107.26 (4-*C*(pz)), not observed (*C*(pz)$_3$), 39.6 (*C*H$_2$C(pz)$_3$), 26.2 (*C*H$_2$CH$_2$C(pz)$_3$), 22.6 (CH$_3$*C*H$_2$), 13.8 (*C*H$_3$CH$_2$), –6.02 ([Al(*C*H$_3$)$_4$], Mg-*C*H$_3$–Mg, 2x Mg-*C*H$_3$-Al, 2x Al(*C*H$_3$)$_3$) ppm. DRIFT: $\tilde{\nu}_{max}$ = 3153 (vw), 2959 (w), 2911 (m), 2875 (w), 2806 (w), 1606 (vw), 1582 (vw), 1531 (w), 1495 (w), 1466 (w), 1390 (w), 1377 (w), 1360 (w), 1305 (vw), 1259 (vw), 1231 (vw), 1190 (m), 1100 (vw), 1076 (m), 1045 (vw), 974 (vw), 839 (m), 761 (vs), 699 (vs), 596 (w) cm^{-1}. $C_{77}H_{99}Mg_2Al_3N_{12}$ (1320.73 g·mol^{-1}) calcd. C 69.94, H 7.55, N 12.71; found C 69.70, H 7.22, N 12.13.

(MeCTp$^{3\text{-}i\text{Pr}}$)Mg(AlMe$_4$)$_2$ (12). To a solution of MeCTp$^{3\text{-}i\text{Pr}}$ (100 mg, 282 μmol) in 2 mL of toluene a solution of **6** (56.0 mg, 282 μmol) in 2 mL of toluene was added dropwise. A white precipitate formed immediately. After removing the solvent under reduced pressure, the crude product was washed with *n*-pentane (3x3 mL) yielding **12** as a white powder (142 mg, 257 μmol, 91%). Colorless crystals of **12** suitable for X-ray diffraction analysis were grown from a 1,2-DFB solution at –40 °C. ^{1}H NMR (400.1 MHz, [D$_6$]benzene/1,2-DFB, 26 °C): δ = 7.77 (dd, 3H, $^3J_{HH}$ = 3.0 Hz, $^4J_{HH}$ = 0.5 Hz, 5-*H*(pz)), 5.78 (d, 9H, $^3J_{HH}$ = 2.9 Hz, 4-*H*(pz)), 3.08 (s, 3H, C*H*$_3$C(pz)$_3$), 2.94 (sept, 3H, C*H*(CH$_3$)$_2$), 0.91 (d, 18 H, $^3J_{HH}$ = 7.0 Hz, CH(C*H*$_3$)$_2$), –0.14 (s, 24H, Mg-C*H*$_3$, Al-C*H*$_3$) ppm. ^{13}C{^{1}H} NMR (100.6 MHz, [D$_6$]benzene/1,2-DFB, 26 °C): δ = 165.2 (3-*C*(pz)), 133.1 (5-*C*(pz)), 104.7 (4-*C*(pz)), 83.3 (*C*(pz)$_3$), 27.8 (*C*H(CH$_3$)$_2$), 24.9 (*C*H$_3$C(pz)$_3$), 22.7 (CH(*C*H$_3$)$_2$), -4.4 (Mg-*C*H$_3$, Al-*C*H$_3$) ppm. DRIFT: $\tilde{\nu}_{max}$ = 3154 (w), 3141 (vw), 3027 (vw), 2969 (w), 2906 (m), 2803 (w), 1532 (m), 1508 (w), 1482 (w), 1462 (w), 1397 (m), 1359 (m), 1303 (w), 1269 (vw), 1215 (s), 1154 (w), 1086 (m), 1070 (w), 1049 (m), 1020 (m), 971 (vw), 930 (vw), 880 (vw), 771 (vs), 691 (vs), 613 (m), 546 (m) cm^{-1}. $C_{34}H_{39}MgAl_2N_6$ (553.05 g·mol^{-1}) calcd. C 60.81, H 9.84, N 15.20; found C 60.28, H 9.64, N 14.42.

Crystallography and Crystal Structure Determinations. Single crystals were grown by standard techniques from saturated solutions (**3d**, diethyl ether; **3e-f**, methyl *tert*-butyl ether (mtbe); **3g-i**, benzene; **3j**, mtbe; **3k**, diethyl ether; **4a**, 1,4-dioxane; **4b**, diglyme; **5**, 1:1 thf / dme; **7**, *n*-hexane; **8**, 1:1 *n*-hexane/toluene; **9a-b**, thf; **9c**, diglyme/*n*-pentane diffusion; **9d**, benzene; **10a-b**, toluene; **11**, benzene; **12**, 1,2-difluorobenzene). Single crystals suitable fofdistinctr X-ray structure analyses were selected in a glovebox and coated with Parabar 10312 (previously known as Paratone N, Hampton Research) and fixed on a nylon loop / glass fiber.

Crystallographic data for compounds **3d-k**, **4a-b**, **5**, **7**, **8**, **9a-d**, **10a-b**, **11**, and **12** were collected on a Bruker APEX DUO instrument equipped with an IμS microfocus sealed tube and

QUAZAR optics for MoK_α radiation (λ = 0.71073 Å). The data collection strategy was determined using COSMO[47] employing ω and ϕ scans. Raw data were processed using APEX[48] and SAINT,[49] corrections for absorption effects were applied using SADABS.[50] The structures were solved by direct methods and refined against all data by full-matrix least-squares methods on F^2 using SHELXTL[51] and Shelxle.[52] All graphics were produced employing ORTEP-3[53] and POV-Ray.[54] Further details of the refinement and crystallographic data are listed in Tables S1-S5 and in the CIF files. CCDCs 1829318-1829338 contain all the supplementary crystallographic data for this paper. These data can be obtained free of charge from The Cambridge Crystallographic Data Centre via www.ccdc.cam.ac.uk/data_request/cif.

Acknowledgements

We are grateful to the German Science Foundation DFG for generous support (Grants:AN 238/15-1).

Conflict of interest

The authors declare no conflict of interest.

Keywords: magnesium • cone angle • trispyrazolylmethane • scorpionate • alkyl

[1] a) V. Grignard, *Compt. rend. Hebd. Séances Acad. Sci.* **1900**, *130*, 1322; b) E. C. Ashby, *Q. Rev. Chem. Soc.* **1967**, *21*, 259-285; c) F. Bickelhaupt, *Angew. Chem. Int. Ed. Engl.* **1974**, *13,* 419-420; *Angew. Chem.* **1974**, *86,* 382; d) H. R. Rogers, C. L. Hill, Y. Fujiwara, R. J. Rogers, H. L. Mitchell, G. M. Whitesides, *J. Am. Chem. Soc.* **1980**, *102*, 217-226; e) F. Bickelhaupt, *Angew. Chem. Int. Ed. Engl.* **1987**, *26,* 990-1005; *Angew. Chem.* **1987**, *99,* 1020; f) F. Bickelhaupt, *J. Organomet. Chem.* **1994**, *475*, 1-14; g) F. Bickelhaupt, *Chem. Soc. Rev.* **1999**, *28*, 17-23; h) P. Knochel, W. Dohle, N. Gommermann, F. F. Kneisel, F. Kopp, T. Korn, I. Sapountzis, V. A. Vu, *Angew. Chem. Int. Ed.* **2003**, *42*, 4302-4320; *Angew. Chem.* **2003**, *115,* 4438-4456; i) R. E. Mulvey, *J. Am. Chem. Soc.* **2008**, *130*, 15217-15217; j) D. Seyferth, *Organometallics* **2009**, *28*, 1598-1605; k) H. B. Kagan, *Angew. Chem. Int. Ed.* **2012**, *51,* 7376-7382; *Angew. Chem.* **2012**, *124,* 7490-7497.

[2] a) P. R. Markies, O. S. Akkerman, F. Bickelhaupt, W. J. J. Smeets, A. L. Spek, *Adv. Organomet. Chem.* **1991**, *32*, 147-226; b) V. C. Gibson, J. A. Segal, A. J. P. White, D. J. Williams, *J. Am. Chem. Soc.* **2000**, *122*, 7120-7121; c) I. J. Blackmore, V. C. Gibson, P. B. Hitchcock, C. W. Rees, D. J. Williams, A. J. P. White, *J. Am. Chem. Soc.* **2005**, *127*, 6012-6020; d) M. R. Crimmin, M. Arrowsmith, A. G. M. Barrett, I. J. Casely, M. S. Hill, P. A. Procopiou, *J. Am. Chem. Soc.* **2009**, *131*, 9670-9685; e) C. Lichtenberg, T. P. Spaniol, I. Peckermann, T. P. Hanusa, J. Okuda, *J. Am. Chem. Soc.* **2013**, *135*, 811-821; f) M. Hatano, T. Horibe, K. Ishihara, *Angew. Chem. Int. Ed.* **2013**, *52,* 4549-4553; *Angew. Chem.* **2013**, *125,* 4647-4651; g) M. H. Chisholm, K. Choojun, A. S. Chow, G. Fraenkel, *Angew. Chem. Int. Ed.* **2013**, *52*; *Angew. Chem.* **2013**, *125,* 3346-3348; h) D. Yang, L. Wang, F. Han, D. Li, D. Zhao, R. Wang, *Angew. Chem. Int. Ed.* **2015**, *54,* 2185-2189; *Angew. Chem.* **2015**, *127,* 2213-2217; i) R. Lalrempuia, C. E. Kefalidis, S. J. Bonyhady, B. Schwarze, L. Maron, A. Stasch, C. Jones, *J. Am. Chem. Soc.* **2015**, *137*, 8944-8947; j) S. Ruccolo, M. Rauch, G. Parkin, *Chem. Sci.* **2017**, *8*, 4465-4474; k) M. Rauch, S. Ruccolo, G. Parkin, *J. Am. Chem. Soc.* **2017**, *139*, 13264-13267; l) A. J. Boutland, A. Carroll, C. Alvarez Lamsfus, A. Stasch, L. Maron, C. Jones, *J. Am. Chem. Soc.* **2017**, *139*, 18190-18193.

[3] a) R. Han, G. Parkin, *Organometallics* **1991**, *10*, 1010-1020; b) R. Han, G. Parkin, *J. Am. Chem. Soc.* **1992**, *114*, 748-757.

[4] O. Michel, H. M. Dietrich, R. Litlabø, K. W. Törnroos, C. Maichle-Mössmer, R. Anwander, *Organometallics* **2012**, *31*, 3119-3127.

[5] S. Trofimenko, *J. Am. Chem. Soc.* **1966**, *88*, 1842-1844.

[6] a) C. J. Snyder, M. J. Heeg, C. H. Winter, *Inorg. Chem.* **2011**, *50*, 9210-9212; b) D. Sambade, G. Parkin, *Polyhedron* **2017**, *125*, 219-229.

[7] K. R. Breakell, D. J. Patmore, A. Storr, *J. Chem. Soc., Dalton Trans.* **1975**, 749-754.

[8] a) D. L. Reger, *Comments Inorg. Chem.* **1999**, *21*, 1-28; b) H. R. Bigmore, S. C. Lawrence, P. Mountford, C. S. Tredget, *Dalton Trans.* **2005**, 635-651.

[9] a) E. E. Pullen, A. L. Rheingold, D. Rabinovich, *Inorg. Chem. Commun.* **1999**, *2*, 194-196; b) E. E. Pullen, D. Rabinovich, C. D. Incarvito, T. E. Concolino, A. L. Rheingold, *Inorg. Chem.* **2000**, *39*, 1561-1567.

[10] A. K. Bartholomew, L. M. Guard, N. Hazari, E. D. Luzik, *Aust. J. Chem.* **2013**, *66*, 1455-1458.

[11] a) M. Garner, J. Reglinski, I. Cassidy, M. D. Spicer, A. R. Kennedy, *Chem. Commun.* **1996**, 1975-1976; b) S. Bakbak, C. D. Incarvito, A. L. Rheingold, D. Rabinovich, *Inorg. Chem.* **2002**, *41*, 998-1001.

[12] a) G. R. Owen, P. Hugh Gould, J. P. H. Charmant, A. Hamilton, S. Saithong, *Dalton Trans.* **2010**, *39*, 392-400; b) G. Nuss, A. Ozwirk, B. N. Harum, G. Saischek, F. Belaj, N. C. Mösch- Zanetti, *Eur. J. Inorg. Chem.* **2012**, *2012*, 4701-4707.

[13] a) G. J. Van Driel, W. L. Driessen, J. Reedijk, *Inorg. Chem.* **1985**, *24*, 2919-2925; b) G. J. Kleywegt, W. G. R. Wiesmeijer, G. J. Van Driel, W. L. Driessen, J. Reedijk, J. H. Noordik, *J. Chem. Soc., Dalton Trans.* **1985**, 2177-2184; c) R. Han, G. Parkin, *J. Am. Chem. Soc.* **1990**, *112*, 3662-3663; d) S. Trofimenko, *Chem. Rev.* **1993**, *93*, 943-980; e) N. Marques, A. Sella, J. Takats, *Chem. Rev.* **2002**, *102*, 2137-2160; f) A. Otero, J. Fernandez-Baeza, A. Antinolo, J. Tejeda, A. Lara-Sanchez, *Dalton Trans.* **2004**, 1499-1510; g) C. Pettinari, R. Pettinari, *Coord. Chem. Rev.* **2005**, *249*, 663-691; h) C. Pettinari, R. Pettinari, *Coord. Chem. Rev.* **2005**, *249*, 525-543.

[14] a) W. Kläui, M. Berghahn, G. Rheinwald, H. Lang, *Angew. Chem. Int. Ed.* **2000**, *39,* 2464-2466; *Angew. Chem.* **2000**, *112,* 2590-2592; b) M. G. Cushion, J. Meyer, A. Heath, A. D. Schwarz, I. Fernández, F. Breher, P. Mountford, *Organometallics* **2010**, *29*, 1174-1190; c) J. Meyer, I. Kuzu, S. González-Gallardo, F. Breher, *Z. Anorg. Allg. Chem.* **2013**, *639*, 301-307.

[15] C. Müller, A. Koch, H. Görls, S. Krieck, M. Westerhausen, *Inorg. Chem.* **2015**, *54*, 635-645.

[16] W. Hückel, H. Bretschneider, *Ber. Dtsch. Chem. Ges.* **1937**, *70*, 2024-2026.

[17] S. Juliá, J. M. del Mazo, L. Avila, J. Elguero, *Org. Prep. Proced. Int.* **1984**, *16*, 299-307.

[18] a) O. Michel, C. Meermann, K. W. Törnroos, R. Anwander, *Organometallics* **2009**, *28*, 4783-4790; b) O. Michel, K. Yamamoto, H. Tsurugi, C. Maichle-Mössmer, K. W. Törnroos, K. Mashima, R. Anwander, *Organometallics* **2011**, *30*, 3818-3825.

[19] K. Ziegler, E. Holzkamp, *Liebigs Ann. Chem.* **1957**, *605*, 93-97.

[20] H. M. Dietrich, G. Raudaschl-Sieber, R. Anwander, *Angew. Chem. Int. Ed.* **2005**, *44,* 5303-5306; *Angew. Chem. Int. Ed.* **2005**, *117,* 5437-5440.

[21] R. Litlabø, M. Zimmermann, K. Saliu, J. Takats, K. W. Törnroos, R. Anwander, *Angew. Chem. Int. Ed.* **2008**, *47,* 9560-9564; *Angew. Chem.* **2008**, *120,* 9702-9706.

[22] C. A. Tolman, *Chem. Rev.* **1977**, *77*, 313-348.

[23] S. Trofimenko, J. C. Calabrese, J. S. Thompson, *Inorg. Chem.* **1987**, *26*, 1507-1514.

[24] J. A. Bilbrey, A. H. Kazez, J. Locklin, W. D. Allen, *J. Comput. Chem.* **2013**, *34*, 1189-1197.

[25] a) A. J. Canty, N. J. Minchin, P. C. Healy, A. H. White, *J. Chem. Soc., Dalton Trans.* **1982**, 1795-1802; b) Daniel L. Reger, Radu F.

Semeniuc, Mark D. Smith, *Eur. J. Inorg. Chem.* **2003**, *2003*, 3480-2494.

[26] a) S. Trofimenko, J. C. Calabrese, P. J. Domaille, J. S. Thompson, *Inorg. Chem.* **1989**, *28*, 1091-1101; b) A.-K. Pleier, H. Glas, M. Grosche, P. Sirsch, W. R. Thiel, *Synthesis* **2001**, *2001*, 0055-0062.

[27] D. L. Reger, T. C. Grattan, *Synthesis* **2003**, *2003*, 0350-0356.

[28] M. A. Esteruelas, L. A. Oro, R. M. Claramunt, C. López, J. L. Lavandera, J. Elguero, *J. Organomet. Chem.* **1989**, *366*, 245-255.

[29] J. L. Atwood, G. D. Stucky, *J. Am. Chem. Soc.* **1969**, *91*, 2538-2543.

[30] D. Pfeiffer, M. J. Heeg, C. H. Winter, *Angew. Chem. Int. Ed.* **1998**, *37,* 2517-2519; *Angew. Chem. Int. Ed.* **1998**, *110,* 2674-2676.

[31] a) A. D. Pajerski, M. Parvez, H. G. Richey, *J. Am. Chem. Soc.* **1988**, *110*, 2660-2662; b) H. Viebrock, U. Behrens, E. Weiss, *Angew. Chem. Int. Ed. Engl.* **1994**, *33,* 1257-1259; *Angew. Chem.* **1994**, *106,* 1364-1365.

[32] a) W. Schlenk, W. Schlenk, *Ber. Dtsch. Chem. Ges.* **1929**, *62*, 920-924; b) W. Schlenk, *Ber. Dtsch. Chem. Ges.* **1931**, *64*, 734-736.

[33] a) M. Parvez, A. D. Pajerski, H. G. Richey, Jnr, *Acta Cryst.* **1988**, *44*, 1212-1215; b) R. Fischer, D. Walther, P. Gebhardt, H. Görls, *Organometallics* **2000**, *19*, 2532-2540; c) M. Gärtner, R. Fischer, J. Langer, H. Görls, D. Walther, M. Westerhausen, *Inorg. Chem.* **2007**, *46*, 5118-5124; d) J. Langer, S. Krieck, R. Fischer, H. Görls, D. Walther, M. Westerhausen, *Organometallics* **2009**, *28*, 5814-5820; e) F. Blasberg, M. Bolte, M. Wagner, H.-W. Lerner, *Organometallics* **2012**, *31*, 1001-1005.

[34] W. Strohmeier, F. Seifert, *Chem. Ber.* **1961**, *94*, 2356-2357.

[35] a) A. C. Cope, *J. Am. Chem. Soc.* **1935**, *57*, 2238-2240; b) C. Stuhl, R. Anwander, *Dalton Trans.* **2018**, DOI: 10.1039/c8dt01542b.

[36] a) H. R. Bigmore, J. Meyer, I. Krummenacher, H. Rüegger, E. Clot, P. Mountford, F. Breher, *Chem. Eur. J.* **2008**, *14*, 5918-5934; b) J. Zagermann, M. C. Kuchta, K. Merz, N. Metzler-Nolte, *Eur. J. Inorg. Chem.* **2009**, *2009*, 5407-5412; c) D. Kratzert, D. Leusser, D. Stern, J. Meyer, F. Breher, D. Stalke, *Chem. Commun.* **2011**, *47*, 2931-2933; d) R. Han, G. Parkin, *J. Organomet. Chem.* **1990**, *393*, C43-C46; e) F. Marchetti, C. Pettinari, R. Pettinari, B. W. Skelton, A. H. White, *Inorg. Chim. Acta* **2009**, *362*, 4480-4485; f) M. G. Ballinas-Lopez, I. I. Padilla-Martinez, F. J. Martinez-Martinez, H. Hopfl, E. V. Garcia-Baez, *Acta Cryst.* **2006**, *62C*, 132-135; g) Y. Sohrin, H. Kokusen, S. Kihara, M. Matsui, Y. Kushi, M. Shiro, *J. Am. Chem. Soc.* **1993**, *115*, 4128-4136.

[37] B. Wrackmeyer, V. Klimkina Elena, *Z. Naturforsch. B* **2008**, *63*, 923-928.

[38] M. Ma, J. Li, X. Shen, Z. Yu, W. Yao, S. A. Pullarkat, *RSC Advances* **2017**, *7*, 45401-45407.

[39] a) A. L. Rheingold, R. L. Ostrander, B. S. Haggerty, S. Trofimenko, *Inorg. Chem.* **1994**, *33*, 3666-3676; b) W. W. Lukens, P. T. Matsunaga, R. A. Andersen, *Organometallics* **1998**, *17*, 5240-5247.

[40] The designation "exact" refers to the mathematical solution for a given molecular structure and chosen set of van der Waals radii; "exact" does not refer to the accuracy of the input structure itself. (*cf.*, Allen et al.)

[41] J. Meyer, I. Kuzu, S. González- Gallardo, F. Breher, *Z. Anorg. Allg. Chem.* **2013**, *639*, 301-307.

[42] R. Han, A. Looney, G. Parkin, *J. Am. Chem. Soc.* **1989**, *111*, 7276-7278.

[43] J. L. Kisko, T. Fillebeen, T. Hascall, G. Parkin, *J. Organomet. Chem.* **2000**, *596*, 22-26.

[44] R. Lalrempuia, A. Stasch, C. Jones, *Chem. Asian J.* **2015**, *10*, 447-454.

[45] M. A. Goodman, M. J. DeMarco, S. E. Tarasek, A. Y. Nazarenko, W. Brennessel, M. S. Goodman, *Inorg. Chim. Acta* **2014**, *423, Part A*, 358-368.

[46] R. I. Yousef, B. Walfort, T. Rüffer, C. Wagner, H. Schmidt, R. Herzog, D. Steinborn, *J. Organomet. Chem.* **2005**, *690*, 1178-1191.

[47] *COSMO v. 1.61*, Bruker AXS Inc., Madison, WI, **2012**.

[48] a) *APEX 2 v. 2012.10_0*, Bruker AXS Inc., Madison, WI, **2012**. b) *APEX 3 v. 2012.10_0*, Bruker AXS Inc., Madison, WI, **2016**.

[49] a) *SAINT v. 8.34A*, Bruker AXS Inc., Madison, WI, **2013**. b) *SAINT v. 8.37A*, Bruker AXS Inc., Madison, WI, **2015**.

[50] a) *SADABS v. 2012/1*, G.M. Sheldrick, AXS Inc., Madison, WI, **2012**. b) *SADABS* L. Krause, R. Herbst-Irmer, G.M. Sheldrick, D. Stalke, *J. Appl. Crystallogr.* **2015**, *48*.

[51] *SHELXTL v. 2012.10_2*, G.M. Sheldrick, Bruker AXS Inc., Madison, WI, **2012**.

[52] C.B. Hübschle, G.M. Sheldrick, B. Dittrich, *J. Appl. Crystallogr.* **2011**, *44*, 1281-1284.

[53] a) L. J. Farrugia, *J. Appl. Crystallogr.* **1997**, *30*, 565. b) L. J. Farrugia, J. Appl. Crystallogr. **2012**, *45*, 849-854.

[54] *POV-Ray v. 3.6*, Persistence of Vision Pty. Ltd., Williamstown, Victoria, Australia, **2004**. http://www.povray.org/.

10.1002/chem.201803067

Entry for the Table of Contents

FULL PAPER

Introducing alkyl substituents at the *C*N3 backbone carbon atom leads to enhanced stabilization of neutral RCTp$^{3\text{-}R'}$ ligands, facilitating the synthesis of a variety of distinct magnesium methyl complexes.

*Christoph Stuhl, Cäcilia Maichle-Mössmer, and Reiner Anwander **

Page No. – Page No.

Magnesium Stung by Non-Classical Scorpionate Ligands: Synthesis and Cone Angle Calculations